Journal of Medicinal Chemistry

Article

pubs.acs.org/jmc

Optimization of Antitrypanosomatid Agents: Identification of Nonmutagenic Drug Candidates with in Vivo Activity

Guzmán Álvarez,[†] Javier Varela,[†] Pablo Márquez,[†] Martín Gabay,[†] Carmen Elena Arias Rivas,[‡] Karina Cuchilla,[‡] Gustavo A. Echeverría,[§] Oscar E. Piro,[§] Marlus Chorilli,[∥] Sandra M. Leal,[⊥] Patricia Escobar,[⊥] Elva Serna,[#] Susana Torres,[#] Gloria Yaluff,[#] Ninfa I. Vera de Bilbao,[#] Mercedes González,*[,†] and Hugo Cerecetto*[,†]

[†]Grupo de Química Medicinal, Laboratorio de Química Orgánica, Facultad de Ciencias−Facultad de Química, Universidad de la República, 11400 Montevideo, Uruguay

[‡]Centro Nacional de Investigaciones Científicas de El Salvador, San Salvador, El Salvador

[§]Departamento de Física, Facultad de Ciencias Exactas, Universidad Nacional de La Plata, and Institute IFLP (CONICET, CCT-La Plata), C.C. 67, 1900 La Plata, Argentina

[∥]Departament of Drugs and Pharmaceuticals, School of Pharmaceutical Sciences, UNESP, Araraquara, Brazil

[⊥]Centro de Investigaciones de Enfermedades Tropicales, Departamento de Ciencias Básicas, Universidad Industrial de Santander, Bucaramanga, Colombia

[#]Departamento de Medicina Tropical, Instituto de Ciencias de la Salud, Universidad Nacional de Asunción, Asunción, Paraguay

Supporting Information

ABSTRACT: Chagas disease, caused by *Trypanosoma cruzi* parasite, was described thousands of years ago. Currently, it affects millions of people, mostly in Latin America, and there are not suitable drugs for treating it. As an attempt to find appropriate drugs to deal with this problem, we report here on the design, synthesis, and characterization of 82 new compounds. Trypanosomicidal behavior in vitro showed more than 20 outstanding derivatives with anti-*Trypanosoma cruzi* activity. Furthermore, we studied the nonspecific toxicity against mammalian cells determining their selectivity and also performed mutagenicity studies. Proof of concept, in vivo studies, was conducted with two of the most promising derivatives (**77** and **80**). They were identified as candidates because they have (i) very simple and cost-effective syntheses; (ii) activity against different stages and strains of the parasite showing excellent in vivo behavior during the acute phase of Chagas disease; and (iii) neither nonspecific toxicity nor mutagenic activity.

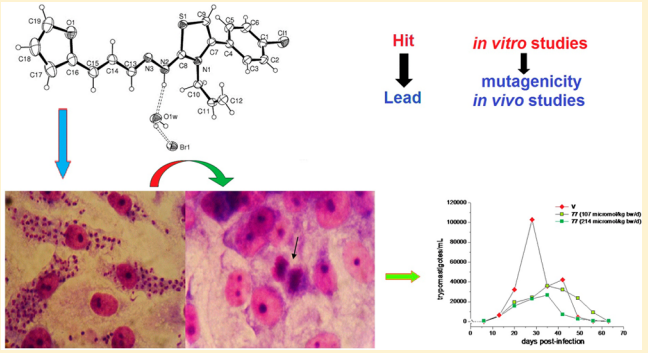

INTRODUCTION

Chagas disease, or American Trypanosomiasis, remains the major parasitic disease burden in Latin America, despite recent advances in the control of its vectorial and transfusional transmission.[1−3] Although excellent chemotherapeutic approaches have been described,[4] still the used pharmacology to control this parasitic infection remains unsatisfactory.[5] The current specific treatments are based on old and quite nonspecific drugs, namely, (±)-3-methyl-*N*-[(1*E*)-5-nitro-2-furylidene]thiomorpholin-4-amine 1,1-dioxide (nifurtimox, recently discontinued by Bayer, **Nfx**, Figure 1a) and *N*-benzyl-2-(2-nitro-1*H*-imidazol-1-yl)acetamide (benznidazole, Roche, **Bnz**) associated with long-term treatments that may give rise to severe side effects. In fact, although **Nfx** and **Bnz** are able to eliminate established parasitemia and to reduce serological titers in acute and early chronic infections, they are not active against all *Trypanosoma cruzi* (*T. cruzi*) strains, have significantly low efficacy in long-term chronic infections,[5] and also are mutagenics.[6] Both drugs act via the reduction of the nitro group, mediated by a type 1 nitroreductase, followed by the fragmentation of the heterocyclic ring, which resulted in the production of toxic metabolites.[7] Side effects of Nifurtimox results from the oxidative damage in the host's tissues and is thus inextricably linked to its antiparasitic activity. Despite these limitations, we have recently shown that 5-nitrofuryl and 5-nitrothienyl derivatives (*E*)-4-allyl-1-(5-nitrofurylidene)-thiosemicarbazide (**I**), (*E*)-4-allyl-1-[3-(5-nitrofuryl)-2*E*-propenylidene]thiosemicarbazide (**II**), and (*E*)-4-allyl-1-(5-nitrothienyl)thiosemicarbazide (**III**) (Figure 1a) possess high

Received: November 19, 2013
Published: April 21, 2014

 © 2014 American Chemical Society

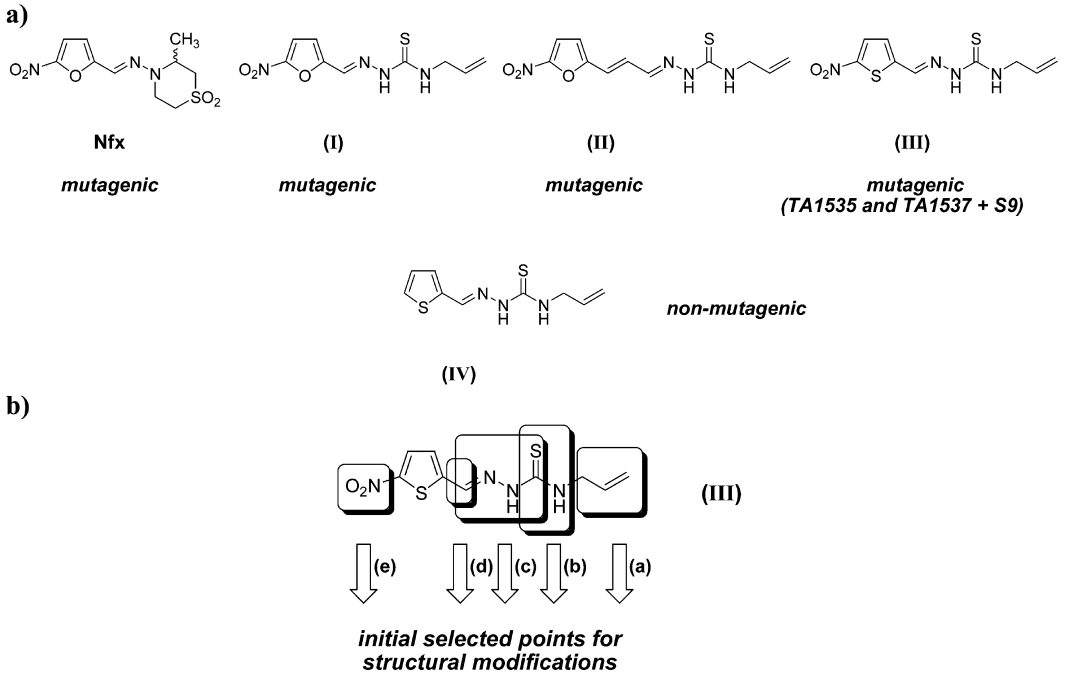

Figure 1. (a) Nifurtimox and other derivatives previously described as *T. cruzi* growth inhibitors. (b) Structural features initially selected for modifications to generate new active anti-*T. cruzi* agents.

and selective anti-*T. cruzi* activity in vitro and in vivo.[8] Furthermore, we have demonstrated that they induce oxidative stress[9] and squalene accumulation in the parasite, hence suggesting that the squalene epoxidase activity inhibition is one of the operative mechanisms of action.[8] However, (**I**) and (**II**) were positive in the Ames test, using *Salmonella typhimurium* TA 98 strain in the presence and absence of S9 from rat liver.[10] Derivative (**III**) was then assessed to confirm the negative results in the other *Salmonella* strains (TA 100, TA 102, TA 1535 and TA 1537) finding mutagenicity against TA 1535 and TA 1573 after treatment with S9. However, the thienyl-analogue (*E*)-4-allyl-1-thienylthiosemicarbazide (**IV**) (Figure 1a) with good in vitro anti-*T. cruzi* activity displayed nonmutagenic properties against the five strains recommended by the Organization for Economic Cooperation and Development (OECD).[11]

Here, we describe the structural modifications done taking as template compound (**III**) (Figure 1b) and the biological studies against different *T. cruzi* strains and stages. The nonspecific toxicity against mammalian cells was studied in order to evaluate the selectivity to the parasites. For the "Hit-to-Lead" phase we performed a series of studies that allowed sieving the best compounds and ensure their use as anti-*T. cruzi* drugs, i.e., mutagenicity, formulation, and stability. Together with the parent compounds (**III**) and (**IV**), two new derivatives were studied in vivo.

METHODS AND RESULTS

"Active-to-Hit" Phase. *Design.* The design of the new derivatives was performed following the biological steps detailed below. They are divided into three stages that involve the preclinical development from synthesis to in vivo evaluation (see Figure S1 in Supporting Information). Step 1 corresponds to the identification of molecular prototypes by in vitro assay in epimastigote forms of the parasite, using as criteria IC_{50} < 4.2 μM to surpass to the following step. In Steps 2 and 3, the leads are selected among those compounds with improved biological activities, both trypanosomicidal activity, IC_{50} in amastigote forms < 20.0 μM, and nonspecific cytotoxicity, selectivity index (mammal cells/amastigotes) > 100 and absence of mutagenicity. Finally, in Step 4, the leads are consolidated by in vivo evaluation. At all points of the procedure, we redesigned the chemicals in a positive feedback between the synthesis and biological activity trying to revert problems like synthesis, solubility, lipophilicity, and stability.

Synthesis. Initially in order to vary the lipophilic properties of the new synthesized derivatives, template-(**III**) was modified at thiosemicarbazone-N^4-nitrogen level (modification (a), Figure 1b), generating derivatives (*E*)-1-(5-nitrothienyl)-thiosemicarbazide, **1**, and (*E*)-4-phenyl-1-(5-nitrothienyl)-thiosemicarbazide, **2** (Table 1), and at the thiophene-thiosemicarbazone linker (modification (d)), generating derivative (*E*)-4-allyl-1-[3-(5-nitrothiophen-2-yl)-2*E*-propenylidene)thiosemicarbazide, **3** (Table 1). The synthetic procedures (Scheme 1)[12,13] generated the desired compounds in good yields. Similar modifications using compound (**IV**) as template (modification (e)) produced compounds **4**−**7** (Table 1, Scheme 1). The other structural modification involved thiosemicarbazone transformation to thiazole system (modification (b)). For this approach different α-haloacetyl reactants were used to generate 4-thiazolidinones (**8**−**16**, Table 1),[14] 4-methylthiazoles (**17**−**21**, Table 1),[15] and 4-arylthiazoles **22**−**38** (Table 1 and Scheme 1).[15] Transformation of thiosemicarbazones into thiadiazoles was accomplished by heating at reflux in acetic anhydride to produce derivatives **39**−**42** (modification (c), Table 1 and Scheme 1) and in the presence of $FeCl_3$ to produce derivative *N*-allyl-5-(5-nitrothiophen-2-yl)-1,3,4-thiadiazol-2-amine, **43** (modification (c), Table 1 and Scheme 1) in good yields (see procedures in Supporting Information).[15]

Given that in the first developed derivatives some compounds do not possess nitro moiety but retained very good biological activity, i.e., derivatives (*E*)-4-allyl-1-[5-

dx.doi.org/10.1021/jm500018m | J. Med. Chem. 2014, 57, 3984−3999

Table 1. First Series of Structural Modifications of Parent Compounds (III) and (IV) and in vitro *T. cruzi* Antiproliferative Activity against Epimastigotes of Tulahuen 2 Strain

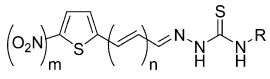

Cpd.	m	n	-R	IC_{50} (μM)[a]
(III)	1	0	$-CH_2CH=CH_2$	4.2 ± 0.6
1	1	0	-H	25 ± 4
2	1	0	-Ph	4.0 ± 0.4
3	1	1	$-CH_2CH=CH_2$	1.2 ± 0.2
(IV)	0	0	$-CH_2CH=CH_2$	7.9 ± 0.8
4	0	0	-Ph	4.7 ± 0.5
5	0	1	$-CH_2CH=CH_2$	> 25± 3
6	0	2	$-CH_2CH=CH_2$	0.60 ± 0.06
7	0	2	-Ph	1.7 ± 0.2

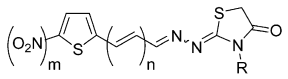

Cpd.	m	n	-R	IC_{50} (μM)[a]
8	1	0	$-CH_2CH=CH_2$	> 25 ± 4
9	1	0	-H	> 25 ± 4
10	1	0	-Ph	13 ± 2
11	1	1	$-CH_2CH=CH_2$	1.3 ± 0.2
12	0	0	$-CH_2CH=CH_2$	> 25 ± 4
13	0	0	-Ph	> 25 ± 4
14	0	1	$-CH_2CH=CH_2$	20 ± 4
15	0	2	$-CH_2CH=CH_2$	> 25 ± 4
16	0	2	-Ph	> 25 ± 4

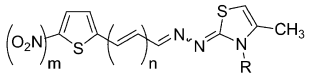

Cpd.	m	n	-R	IC_{50} (μM)[a]
17	1	0	$-CH_2CH=CH_2$	20 ± 3
18	1	1	$-CH_2CH=CH_2$	10 ± 1
19	0	0	$-CH_2CH=CH_2$	> 25 ± 4
20	0	0	-Ph	> 25 ± 3
21[b]	0	1	$-CH_2CH=CH_2$	> 25± 3

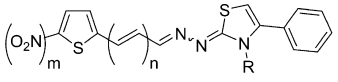

Cpd.	m	n	-R	IC_{50} (μM)[a]
22*EE*	1	0	$-CH_2CH=CH_2$	20 ± 3
22*EZ*				6 ± 1
23	1	0	-Ph	> 25 ± 4
24	0	0	$-CH_2CH=CH_2$	> 25 ± 4
25[b]	0	1	$-CH_2CH=CH_2$	> 25 ± 4

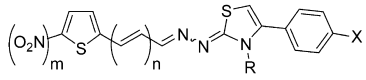

Cpd.	m	n	-R	-X	IC_{50} (μM)[a]
26[b]	1	0	$-CH_2CH=CH_2$	$-OCH_3$	8 ± 1
27	1	0	$-CH_2CH=CH_2$	-Cl	14 ± 2
28	1	0	-H	-Cl	4.9 ± 0.5
29	1	0	$-CH_2CH=CH_2$	$-NO_2$	10 ± 1
30	1	1	$-CH_2CH=CH_2$	-Cl	10 ± 1
31	1	1	$-CH_2CH=CH_2$	$-NO_2$	3.3 ± 0.5

Cpd.	m	n	-R	-X	IC_{50} (μM)[a]
32	0	0	$-CH_2CH=CH_2$	-Cl	> 25 ± 4
33[b]	0	1	$-CH_2CH=CH_2$	$-OCH_3$	> 25 ± 4
34[b]	0	1	$-CH_2CH=CH_2$	-Cl	> 25 ± 4
35	0	1	$-CH_2CH=CH_2$	-Br	> 25 ± 4
36[b]	0	1	$-CH_2CH=CH_2$	$-NO_2$	> 25 ± 4
37[b]	0	2	$-CH_2CH=CH_2$	-Cl	11 ± 1

Cpd.	Structure	IC_{50} (μM)[a]
38[b]	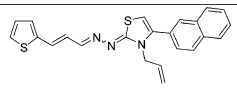	> 25 ± 4
39	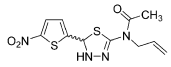	> 25 ± 3
40	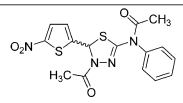	2.9 ± 0.3

Cpd.	Structure	IC_{50} (μM)[a]
41	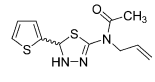	> 25 ± 3
42	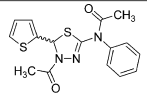	> 25 ± 4
43	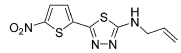	12 ± 2

[a]Each compound concentration was evaluated in duplicate. [b]This compound is shown as the base form; however, it was isolated and evaluated as the hydrobromide form (see text).

dx.doi.org/10.1021/jm500018m | *J. Med. Chem.* 2014, 57, 3984−3999

Scheme 1. Synthetic Procedures Used to Prepare the New Derivatives (See Procedures in Supporting Information); Y* = Range of Yields

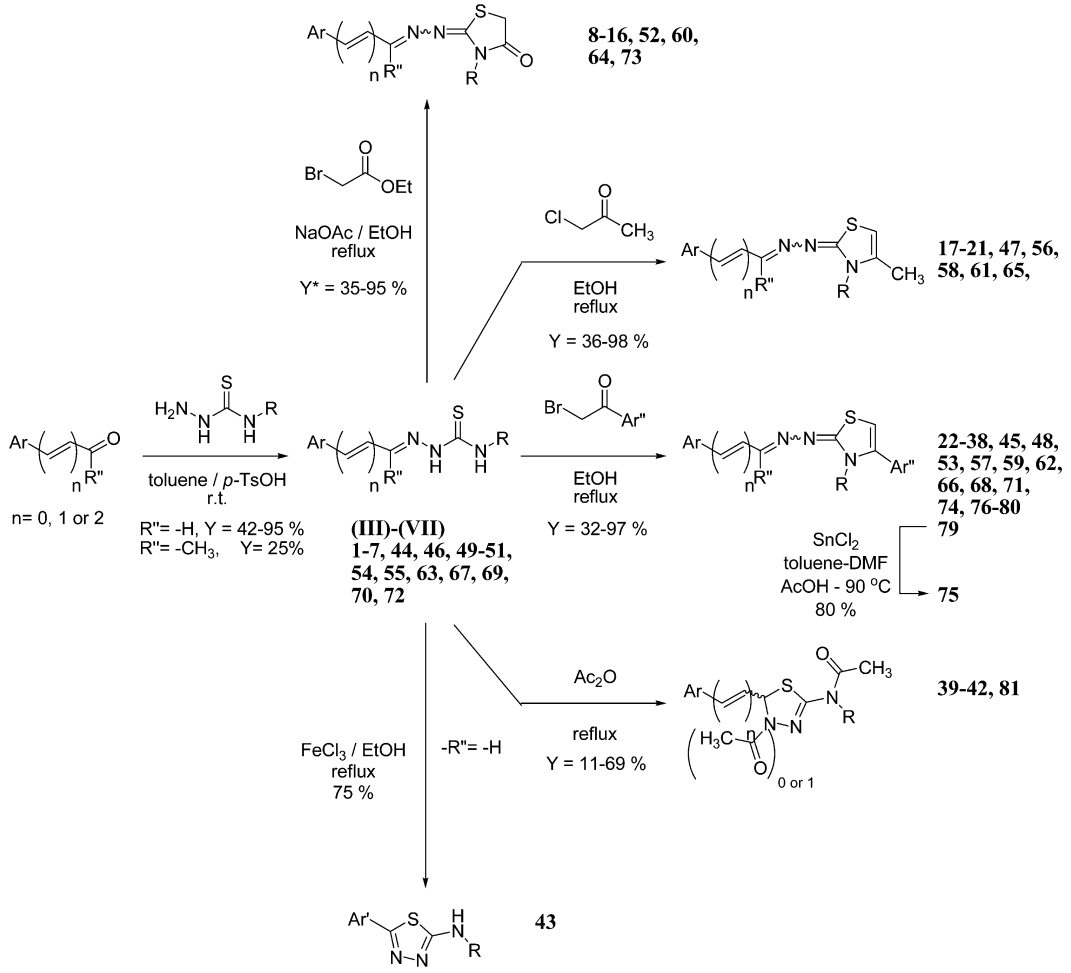

(thiophen-2-yl)penta-2*E*,4*E*-dienylidene]thiosemicarbazide, **6**, and (*E*)-4-phenyl-1-[5-(thiophen-2-yl)penta-2*E*,4*E*-dienylidene)thiosemicarbazide, **7** (with IC_{50}s lower than the corresponding value for (**III**), Table 1), we decided to investigate the relevance of the 5-nitrothienyl group as pharmacophore for anti-*T. cruzi* activity. For that purpose we planned a new series of derivatives where the main modification was the substitution of 5-nitrothienyl moiety by different aryl groups. Additionally, modifications (a), (b), and (d) (Figure 1b) were also included in these series of studies (Table 2). Compounds **44**−**74** were synthesized following the general procedures shown in Scheme 1.

During the analysis of biological activities, we observed that derivative 1*Z*-[3-allyl-4-phenylthiazol-2(3*H*)-ylidene]-2*E*-[3-(2-furyl)-2*E*-propenylidene]hydrazine, **62**, a 2-furyl containing 4-phenylthiazole derivative, displayed excellent in vitro activity. This observation encouraged us to develop a third series of compounds (**75**−**81**, Table 3) using this derivative as a new structural prototype.

All the compounds were characterized by ^{1}H NMR and ^{13}C NMR spectroscopy and also by MS (see results in Supporting Information). The purity was established by TLC and microanalysis. Stereochemistry of the exocyclic double bond (Figure 2a) for thiazole derivatives (**8**−**38**, **45**, **47**, **48**, **52**, **53**, **56**−**59**, **60**−**62**, **64**−**66**, **68**, **71**, and **73**−**80**) were established using NOE-diff experiments. In general, the *EZ* isomers (nomenclature according to Figure 2a) were either the most abundant or the exclusive isolated species. In the case of derivative 1-(3-allyl-4-phenylthiazol-2(3*H*)-ylidene)-2-(5-nitro-2-thienyl)hydrazine, **22**, each isomer, *EE* and *EZ*, was isolated, hence confirming the NOE-diff analysis (see Figure S2 in Supporting Information). Stereochemistry around chiral center in derivatives **39**−**42** and **81** was not determined.

According to spectroscopic data, when -R = -H (derivatives 2-[2*E*-(5-nitro-2-thienyl)hydrazinyl]thiazol-4(5*H*)-one, **9**, and [4-(4-chlorofenyl)]-2-[2*E*-(5-nitro-2-thienyl)hydrazinyl]-thiazol-4(5*H*)-one, **28**), the thiazole system existed as *NH* exocyclic tautomeric form (Figure 2b). The thiazoles that precipitated from the mixture of reactions (**21**, **25**, **26**, **33**, **34**, **36**−**38**, **48**, **57**, **62**, 71, **76**−**78**, and **80**) were obtained as the corresponding hydrobromides. Adequate single crystals were obtained for derivative 1*Z*-[3-allyl-4-(4-chlorophenyl)thiazol-2(3*H*)-ylidene]-2*E*-[3-(2-furyl)-2*E*-propenylidene] hydrazine, 77, to analyze its structure by X-ray diffraction methods (Figure 2c). In the solid state, this compound existed at the 2-aminothiazolium tautomeric form (Figure 2d).

Biological Characterization. In Vitro Anti-T. cruzi Activity. The new developed derivatives were initially tested in vitro against the epimastigote form of *T. cruzi*, Tulahuen 2 strain. The existence of the epimastigote form of *T. cruzi* as an obligate mammalian intracellular stage has been reviewed and confirmed.[17] The compounds were incorporated into the

dx.doi.org/10.1021/jm500018m | *J. Med. Chem.* 2014, 57, 3984−3999

Table 2. Second Series of Structural Modifications from Parent Compound (III) and Derivatives 6 and 7 and in Vitro *T. cruzi* Antiproliferative Activity against Epimastigotes of Tulahuen 2 Strain

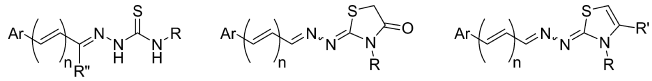

structure type (A) structure type (B) structure type (C)

Cpd.	structure type	-Ar	*n*	-R″	-R	-R′	IC_{50} (μM)[a]
44	(A)	-Ph	0	-H	-Ph		19 ± 2
45	(C)	-Ph	0	-H	-Ph	-Ph	>25 ± 3
46	(A)	-Ph	1	-H	$-CH_2CH{=}CH_2$		6.6 ± 0.7
47	(C)					$-CH_3$	>25 ± 3
48[b]						-Ph	>25 ± 3
49	(A)	-*p*-OHPh	0	-H	$-CH_2CH{=}CH_2$		>25 ± 3
50	(A)	-*p*-(SCH_3)Ph	0	-H	$-CH_2CH{=}CH_2$		10 ± 1
51	(A)	-*p*-ClPh	0	-H	$-CH_2CH{=}CH_2$		11 ± 1
52	(B)						>25 ± 4
53	(C)					-*p*-ClPh	>25 ± 4
54	(A)	-3,4-($-OCH_2O-$)Ph	0	-H	$-CH_2CH{=}CH_2$		>25 ± 3
55	(A)	-5-bromo-3-pyridinyl	0	-H	$-CH_2CH{=}CH_2$		>25 ± 4
(**V**)[c]	(A)	2-furyl	0	-H	$-CH_2CH{=}CH_2$		>25 ± 3
56	(C)					$-CH_3$	>25 ± 3
57[b]						-Ph	>25 ± 3
58	(C)	-5-(SO_3H)-2-furyl				$-CH_3$	>25 ± 3
59						-Ph	>25 ± 3
(**VI**)[c]	(A)	2-furyl	1	-H	$-CH_2CH{=}CH_2$		7.0 ± 0.7
60	(B)						>25 ± 3
61	(C)					$-CH_3$	>25 ± 3
62[b]						-Ph	3.2 ± 0.4[d]
63	(A)				-Ph		11 ± 1
64	(B)						>25 ± 3
65	(C)					$-CH_3$	25 ± 3
66[b]						-Ph	5.0 ± 0.6
67	(A)	-3-thienyl	0	-H	$-CH_2CH{=}CH_2$		>25 ± 3
68	(C)	-3-thienyl	0	-H	$-CH_2CH{=}CH_2$	-*p*-ClPh	14.6 ± 0.3
69	(A)	-2-benzo[*b*]furyl	0	$-CH_3$	$-CH_2CH{=}CH_2$		>25 ± 3
70	(A)	-2-naphtyl	0	-H	$-CH_2CH{=}CH_2$		5.4 ± 0.5
71[b]	(C)	-4-quinolinyl	0	-H	$-CH_2CH{=}CH_2$	-Ph	>25 ± 3
72	(A)						17 ± 2
(**VII**)[e]	(A)	-2,3-dimethyl-1,4-dioxide-6-quinoxalinyl	0	-H	$-CH_2CH{=}CH_2$		>25 ± 3
73	(B)						>25 ± 3
74	(C)					-*p*-ClPh	15 ± 2

[a]Each compound concentration was evaluated in duplicate. [b]This compound is shown as the base form; however, it was isolated and evaluated as the hydrobromide form (see text). [c]Product previously described.[8b] [d]The compound was also evaluated against *T. cruzi* epimastigote Dm 28c clone (IC_{50} of 4.0 ± 0.3 μM). [e]Product previously described.[16]

biological milieu at 25 μM, and their ability to inhibit growth of the parasite was evaluated in comparison with that of the control (no drug added to the milieu) on day 5 (growth exponential phase). **Nfx** and **Bnz** were used as the trypanosomicidal reference drugs. The IC_{50} concentrations (50% inhibitory concentration) were assessed for **Nfx** and **Bnz**, 8 ± 1 and 7 ± 1 μM, respectively, and the most active derivatives (Tables 1, 2, and 3). From the first and second series of chemical modifications, more active derivatives, than the nitrothienyl-, (**III**), and the thienyl-, (**IV**), parent compounds (IC_{50} of 4.2 ± 0.6 and 7.9 ± 0.8 μM, respectively), were obtained. For example, the nitrothienyl-thiosemicarbazone **3** (IC_{50} = 1.2 ± 0.2 μM), the nitrothienyl-thiazolidinone 2*Z*-[3-(5-nitrothiophen-2-yl)-2*E*-propen-1*E*-ylidenehydrazono]-3-allylthiazolidin-4-one, **11** (IC_{50} = 1.3 ± 0.2 μM), the nitrothienyl-thiazole 1*E*/*Z*-[3-allyl-4-(4-nitrophenyl)thiazol-2(3*H*)-ylidene]-2*E*-[3-(5-nitrothiophen-2-yl)-2*E*-propenylidene]hydrazine, **31** (IC_{50} = 3.3 ± 0.5 μM) or the nitrothienyl-thiadiazole *N*-[4-acetyl-5-(5-nitrothiophen-2-yl)-4,5-dihydro-1,3,4-thiadiazol-2-yl]-*N*-phenylacetamide, **40** (IC_{50} = 2.9 ± 0.3 μM), and the thienyl-thiosemicarbazone **6** (IC_{50} = 0.60 ± 0.06 μM) or the furyl-thiazole **62** (IC_{50} = 3.2 ± 0.4 μM).

From the analysis of the biological response of the first 74 studied derivatives, the previous described compounds (**III**)−(**VII**), (Tables 1 and 2), and the results against amastigotes forms (Table 4), we redirected our synthetic strategies trying to improve the activity of derivative **62**. This derivative, without the potential mutagenophore nitro-moiety, was twice as much more active against epimastigotes than the corresponding parent compound (**VI**) (Table 2). The cyclization of (**VI**) to the thiazolidinone **60**, to the methylthiazole 1*E*/*Z*-[3-allyl-4-methylthiazol-2(3*H*)-ylidene]-2*E*-[3-(2-furyl)-2*E*-propenylidene]hydrazine, **61**, or to the thiadiazole *N*-[4-acetyl-

dx.doi.org/10.1021/jm500018m | *J. Med. Chem.* 2014, 57, 3984−3999

Table 3. Third Series of Structural Modifications of Structural Prototype 62 and in Vitro *T. cruzi* Antiproliferative Activity against Epimastigotes of Tulahuen 2 Strain

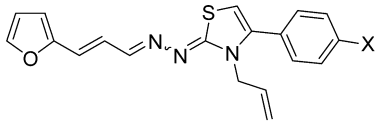

Cpd.	-X	IC_{50} (μM)[a]
75	$-NH_2$	9.0 ± 0.9
76[b]	$-OCH_3$	4.9 ± 0.6
77[b]	-Cl	1.3 ± 0.2

Cpd.	-X	IC_{50} (μM)[a]
78[b]	-Br	2.9 ± 0.4
79[b]	$-NO_2$	> 25 ± 3

Cpd.	Structure	IC_{50} (μM)[a]
80[b]	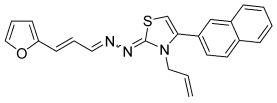	2.4 ± 0.3

Cpd.	Structure	IC_{50} (μM)[a]
81	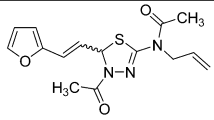	> 25 ± 3

[a]Each compound concentration was evaluated in duplicate. [b]This compound is shown as the base form; however, it was isolated and evaluated as the hydrobromide form (see text).

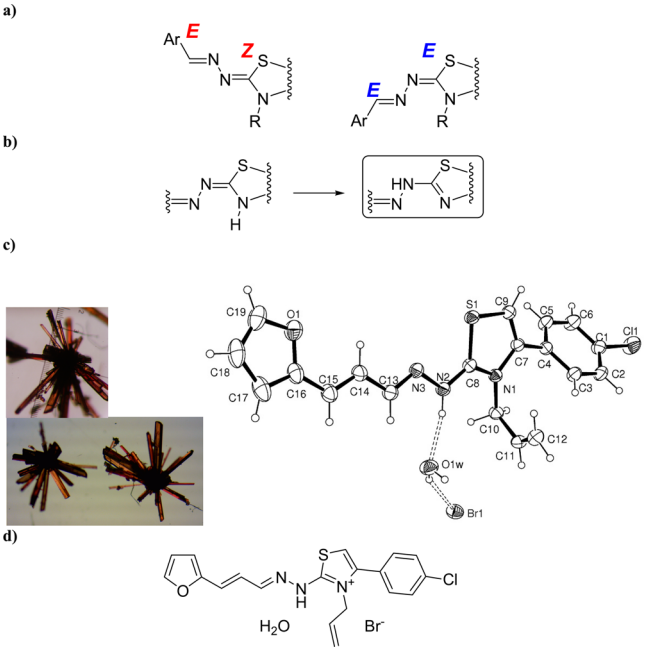

Figure 2. (a) Possible configurations around exocyclic double bond for thiazole derivatives. (b) Tautomeric form observed (right structure), in solution, for derivatives **9** and **28**. (c) Photographs of derivative 77 single crystals and drawing of the corresponding molecular model showing the labeling of the non-H atoms and their displacement ellipsoids at the 30% probability level. Dashed lines indicate intermolecular H-bonds. (d) 2-Aminothiazolium tautomeric form of derivative 77 observed in the solid state.

5-[2-(furan-2-yl)-1*E*-ethenyl]-4,5-dihydro-1,3,4-thiadiazol-2-yl]-*N*-allylacetamide, **81** (Table 3), was conducted to compounds with lower anti-*T. cruzi* activity. However, the arylthiazoles **76**–**78** were more active than (**VI**) where derivatives 1*Z*-[3-allyl-4-(4-chlorophenyl)thiazol-2(3*H*)-ylidene]-2*E*-[3-(2-furyl)-2*E*-propenylidene]hydrazine, 77 (IC_{50} = 1.3 ± 0.2 μM), and 1*Z*-[3-allyl-4-(2-naphthyl)thiazol-2(3*H*)-ylidene]-2*E*-[3-(2-furyl)-2*E*-propenylidene]hydrazine, **80** (IC_{50} = 2.4 ± 0.3 μM), were more active than the new prototype phenyl-thiazole **62** (Table 3).

The above studies were followed (according to Figure S1, Supporting Information) by the assessment of the activity of selected derivatives against the parasitic relevant form for the disease, namely, the amastigote form, using Sylvio X-10 strain (Table 4).[18] Acetyl-derivatives **39**–**42** were not included in this study due to the low stability in biological milieu (see, as an example, the results with the active derivative **40**; Figure S3, Supporting Information). Except for some derivatives (**6**, 7, **10**, **22*EZ***, **26**, **27**, **29**, **32**, **37**, and **61**), the developed compounds showed similar behavior in both forms of the parasite. Sixteen in 26, 61.5%, possessed the same tendency of activities in both parasitic forms (Figure S4, Supporting Information). Additionally, 87.5% of the most active derivatives, $IC_{50} \leq 20$ μM, in amastigote form possessed $IC_{50} \leq 20$ μM in the epimastigote one (Figure S4, Supporting Information). The most active derivatives were the furyl containing aryl-thiazole **62**, 77, and **80**. They eradicated near to 100% of the amastigotes parasites at doses at least one and a half lower than the corresponding doses for **Nfx** (see IC_{90} values in Table 4) having derivative 77 with the best behavior with an IC_{90} in amastigotes of 310 nM. In fact, these compounds were able to eradicate the amastigotes form into Vero cells after 72 h of treatment (Figure 3).

Additionally, derivative 77 was tested in vitro against the bloodstream trypomastigote form of *T. cruzi*, Y strain. The compound was incorporated into the biological milieu at 25 μM producing 70% of parasite growth inhibition, in comparison to that of the control (no drug added to the milieu), after 48 h of incubation. **Bnz**, used as the trypanosomicidal reference drug, produced 90% of parasite growth inhibition in the same conditions.

In Vitro Nonspecific Mammal Cytotoxicity. To explore the selectivity of these new derivatives against *T. cruzi* we evaluated the in vitro nonspecific mammal cytotoxicity, using VERO monkey kidney epithelial cells, human red blood cells, and in

dx.doi.org/10.1021/jm500018m | *J. Med. Chem.* 2014, 57, 3984–3999

Table 4. Biological Characterization of Developed Derivatives Against Amastigotes Form, Sylvio X-10 Strain, and Mammal Cells

Cpd.	IC_{50} (μM)[a]	IC_{90} (μM)[a]	SI_V[b]	SI_R[c]	SI_J[d]
(**III**)	19.4 ± 2.2	>25 ± 4	100	*e*	
2	4.1 ± 0.1	14.4 ± 0.4	20		
3	1.29 ± 0.04	4.06 ± 0.15	60	82	
4				21[f]	
6	>25 ± 4	>25 ± 4			
7	>25 ± 4	>25 ± 4			
8	>25 ± 4	>25 ± 4			
10	>25 ± 4	>25 ± 4			
11	2.8 ± 0.3	9.9 ± 4.3	80	28	
17	2.55 ± 0.06	9.30 ± 0.24			
18	10.5 ± 2.8	21.2 ± 2.4			
19	>25 ± 4	>25 ± 4			
21					<7[f]
22*EZ*	25 ± 4	>25 ± 4	5		
26	>25 ± 4	>25 ± 4			
27	>25 ± 4	>25 ± 4			
28	*g*	*g*			
29	>25 ± 4	>25 ± 4			
30	16.9 ± 0.7	25.36 ± 0.25			
31	8.2 ± 0.6	>25 ± 4	13		
32	8.0 ± 1.2	10.2 ± 0.5			
37	>25 ± 4	>25 ± 4			
40	*g*	*g*		3[f]	
43	5.0 ± 0.5	15.9 ± 9.6	50		
61	6.3 ± 0.6	51 ± 22			
62	<0.24 ± 0.02	1.30 ± 0.02	>1000	>196	>120
77	<0.25 ± 0.02	0.31 ± 0.02	>1000	>234	>200
80	<0.21 ± 0.02	1.4 ± 0.2	>1000		>120
Bnz	3.3 ± 0.3		300		
Nfx	0.45 ± 0.01	2.4 ± 0.2	200	150	200
AmpB[h]	1.1 ± 0.1			10	

[a]Each compound concentration was evaluated in quadruplicate. [b]SI_V: selectivity index, $IC_{50,VERO\ cells}/IC_{50,T.\ cruzi\ (amastigotes,\ Sylvio\ X\text{-}10)}$. [c]$SI_R$: selectivity index, $IC_{50,human\ blood\ red\ cells}/IC_{50,T.\ cruzi\ (amastigotes,\ Sylvio\ X\text{-}10)}$. [d]$SI_J$: selectivity index, $IC_{50,J774.1\ mouse\ macrophages}/IC_{50,T.\ cruzi\ (amastigotes,\ Sylvio\ X\text{-}10)}$. [e]Blank cells = not studied. [f]Selectivity index defined as $IC_{50,mammal\ cells}/IC_{50,T.\ cruzi\ (epimastigotes,\ Tulahuen\ 2)}$. [g]The derivative was not evaluated in this assay due to its high cytotoxicity against VERO cells (more than 50% of VERO-growth inhibition at the lower evaluated concentration, 25 μM). [h]AmpB: amphotericin B.

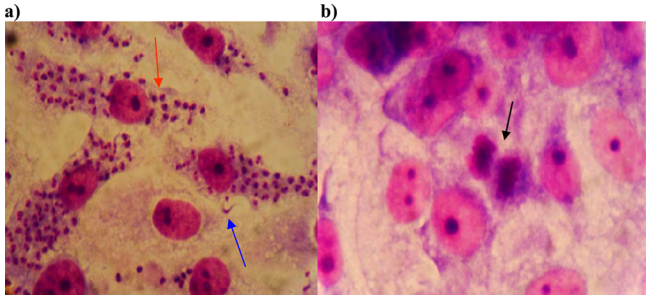

Figure 3. (a) Optic microscopy of VERO cells infected with *T. cruzi* (Sylvio X-10 strain), amastigotes (red arrow), and typomastigotes (blue arrow) are visualized. (b) Optic microscopy of treated cells with 5 μM of derivative **77** after 72 h of incubation. The cells are free of infection and undergoing cellular division (black arrow).

some cases J774.1 mouse macrophages (Table S1, Supporting Information). The new developed compounds were selected according to their anti-*T. cruzi* activity and trying to cover a wide range of structural characteristics. The selectivity indexes (SI, Table 4) were expressed as the ratio between IC_{50} in mammal cells and IC_{50} in *T. cruzi* amastigotes Sylvio X-10 strain.[19] Derivatives **62**, **77**, and **80** displayed low cytotoxicity against mammal cells with adequate selectivity indexes toward the parasite. The worst selective derivative and most cytotoxics against VERO cells were the nitro-thienyl derivatives **22*EZ***, [4-(4-chlorophenyl)]-2-[2*E*-(5-nitro-2-thienyl)hydrazinyl]thiazol-4(5*H*)-one (**28**), and **40**.

"Hit-to-Lead" Phase. *Mutagenicity Studies.* The method of direct incubation in plate[20] using culture of *Salmonella typhimurium* TA 98 strain was initially performed on some selected derivatives and **Nfx**. The influence of metabolic activation was tested by adding S9 fraction of mouse liver. Positive controls of 4-nitro-*o*-phenylendiamine and 2-amino-fluorene were run in parallel. The revertant number was manually counted and compared to the natural revertant (Table 5). The compound is considered mutagenic when the number

Table 5. Mutagenic Properties of New Derivatives and Nfx on TA98 *S. typhimurium* Strain

		mutagenicity[a,b]	
Cpd.	*D*[c]	without S9	with S9
3	3, 9, 27, 83, 250	(+)	(+)
5	5, 15, 44, 133, 400	(−)	(−)
6	6, 19, 56, 167, 500	(−)	(−)
11	0.02, 0.07, 0.2, 0.7, 2	(+)	(−)
14	5, 15, 44, 133, 400	(+)	(+)
17	0.005, 0.01, 0.04, 0.13, 0.4	(−)	(−)
18	0.005, 0.01, 0.04, 0.13, 0.4	(−)	(−)
21	0.3, 1, 4, 13, 40	(−)	(−)
31	0.04, 0.1, 0.4, 1.3, 4	(+)	(+)
37	3.1, 9.3, 28, 83, 250	(−)	(−)
40	0.005, 0.01, 0.04, 0.13, 0.4	(±)[d]	(−)
43	0.05, 0.1, 0.4, 1.3, 4	(−)	(−)
61	6, 19, 56, 167, 500	(−)	(−)
62	3.1, 9.3, 28, 83, 250	(−)	(−)
75	0.04, 0.1, 0.4, 1.3, 4	(−)	(−)
76	5, 15, 44, 133, 400	(−)	(−)
77	5, 15, 44, 133, 400	(−)	(−)
78	5, 15, 44, 133, 400	(−)	(−)
79	5, 15, 44, 133, 400	(+)	(+)
80	6, 19, 56, 167, 500	(−)	(−)
Nfx	0.5, 1, 3, 10, 30	(+)	(+)

[a]The results are the means of two independent experiments. [b]Mutagenicity, according to ref 21 (see text). (+), mutagenic; (−), nonmutagenic. [c]*D*: studied doses (in μg/plate). [d](±): At the higher studied dose the revertant level is twice the spontaneous frequencies.

of revertant colonies is at least twice the spontaneous revertant frequencies for at least two consecutive dose levels.[21] The maximum assayed doses were determined according to toxic effect on *S. typhimurium*. Fifty-six percent of the nitro containing derivatives were mutagenic in at least one experimental condition. The nitro group is located in the heterocyclic-moiety like in **3**, 2*Z*-[3-(5-nitrothiophen-2-yl)-2*E*-propen-1*E*-ylidenehydrazono]-3-allylthiazolidin-4-one, **11**, *N*-[4-acetyl-5-(5-nitrothiophen-2-yl)-4,5-dihydro-1,3,4-thiadiazol-2-yl]-*N*-phenylacetamide, and **Nfx** or in another position of the

dx.doi.org/10.1021/jm500018m | *J. Med. Chem.* 2014, 57, 3984−3999

Table 6. Mutagenic Properties of Prototype 61 and Derivatives 62, 77, and 80 on *S. typhimurium* Strains Recommended by OECD

		TA100[a,b]		TA102[a,b]		TA1535[a,b]		TA1537[a,b]	
Cpd.	D^c	(−) S9	(+) S9	(−) S9	(+) S9	(−) S9	(+) S9	(−) S9	(+) S9
61	0.003, 0.007, 0.02, 0.06, 0.2[d]	(−)	(−)	(−)	(−)	(−)	(−)	(−)	(−)
62	0.06, 0.19, 0.5, 1.7, 5	(−)	(−)	(−)	(−)	(−)	(−)	(−)	(−)
77	3.09, 9.26, 27.77, 83.33, 250[e]	(−)	(−)	(−)	(−)	(−)	(−)	(−)	(−)
80	6, 19, 56, 167, 500	(−)	(−)	(−)	(−)	(−)	(−)	(−)	(−)

[a]The results are the means of two independent experiments. [b]Mutagenicity, according to ref 21 (see text). (+), mutagenic; (−), nonmutagenic. [c]*D*: studied doses (in μg/plate). [d]For TA 100, the used doses were 3.09, 9.26, 27.77, 83.33, and 250 μg/plate. [e]For TA 100, the used doses were 0.003, 0.007, 0.02, 0.06, 0.2 μg/plate.

structure, like in 1*Z*-[3-allyl-4-(4-nitrophenyl)thiazol-2(3*H*)-ylidene]-2*E*-[3-(2-furyl)-2*E*-propenylidene]hydrazine, **79**, or in both, like in **31**. Only 8% of derivatives without nitro-moiety was mutagenic in both conditions: derivative 3-allyl-2*E*/*Z*-[2*E*-[3-(thiophen-2-yl)-2*E*-propenylidene]hidrazono] thiazolidin-4-one, **14**.

To complete the OECD recommendations, some of the most relevant derivatives, **61**, **62**, **77**, and **80**, were evaluated against *S. typhimurium* TA 100, TA 102, TA 1535, and TA 1537 strains without and with metabolic activation (Table 6). Positive controls, 4-nitro-*o*-phenylendiamine and 2-amino-fluorene for TA 100, sodium azide, and 2-aminoantracene for TA 102, TA 1535, and TA 1537, were run in parallel. The four studied compounds fulfilled the OECD requirements.

Formulation Studies. For the in vivo studies the compounds were initially suspended in a mixture of saline/Tween 80 (4:1, v:v) as vehicle (V1) in order to employ an aqueous-like formulation. However, the use of different doses was limited by the low suspension ability of V1; additionally, the biological results were very erratic using this vehicle.

Thus, studies to improve vehicle system to dispose adequately of the compounds were undertaken. To this purpose, we selected microemulsion as vehicle.[22] This is a mixing of water and oil stabilized by a surfactant systemwhich is thermodynamically stable and, depending on composition, exhibits a wide range of nanostructures.

Consequently, the second vehicle (V2) was a microemulsion composed of cholesterol (10%) as oil phase, the surfactant (soya phosphatidylcholine/sodium oleate/polyoxyl-40 hydrogenated castor oil (3:6:8, 10%)), and phosphate buffer pH 7.4 (80%) as aqueous phase.[23] This vehicle generated a homogeneous and stable suspension for, at least, both one month at 4 °C and more than 20 days at 30 °C.

Stability Studies. We analyzed the stability, of selected derivatives, i.e., 1*Z*-(3-allyl-4-methylthiazol-2(3*H*)-ylidene)-2*E*-(2-thienyl)hydrazine (**19**), **61**, **62**, 1*Z*-[3-allyl-4-(4-methoxyphenyl)thiazol-2(3*H*)-ylidene]-2*E*-[3-(2-furyl)-2*E*-propenylidene]hydrazine (**76**), **77**, 1*Z*-[3-allyl-4-(4-bromophenyl) thiazol-2(3*H*)-ylidene]-2*E*-[3-(2-furyl)-2*E*-propenylidene]hydrazine (**78**), and **80**, on simulated physiological conditions, namely, aqueous solution at different pHs,[19c] in the presence of hepatic rat cytosolic and microsomal fractions,[24] and in the vehicle V2 (Figure 4). Except for thiophene derivative **19**, all the compounds were stable or partially stable, remaining more than 95% of the derivative at the end of the assay, during 1 h on aqueous solution pH 6.0, 7.4, and 9.0. On aqueous solution at pH 1.0, **61**, **62**, and **77** derivatives showed some degree of instability, remaining near to 90% of the derivative at the end of the assay, and no attempt to isolate the decomposition products was done. Derivatives **19**, **77**, and **80** were stable on liver metabolic fraction for 1 h at 37 °C. Additionally, derivatives **62**, **77**, and **80** were stable in V2 during storage at 4 °C.

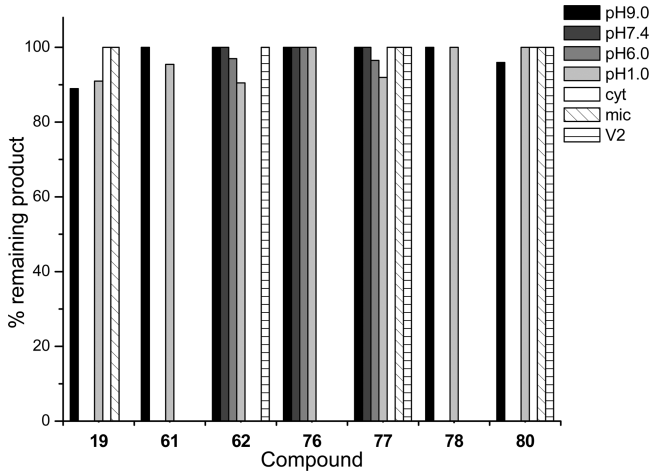

Figure 4. Stability of selected compounds in simulated physiological conditions and in storage formulation. For the studies in aqueous milieu and in the presence of cytosolic (cyt) and microsomal (mic) fractions, the assays were conducted over a period of 1 h, at 37 °C, while the storage studies on the vehicle (V2) were conducted over a period of 1 week, at 4 °C.

Proof of Concept: in Vivo anti-T. cruzi Studies. Oral Effects on Uninfected Mice. Parent compounds (**III**) and (**IV**) and thiazoles **77** and **80** were given orally and daily, by intragastric gavage, to uninfected female BALB/c mice (n = 2/group) at 100 mg/kg body weight/day, in V1, for 14 days. Mice were weighted and monitored daily, and at the end of the experiments the animals were sacrificed and necropsies were done in order to evaluate macroscopically the organ status. Neither mortality nor signs associated with toxicity were observed.

Treatment of T. cruzi Infected Mice. Parent compounds (**III**) and (**IV**) and thiazoles **77** and **80** were evaluated in vivo in murine models of acute Chagas' disease. **Bnz** was used as the in vivo active reference drug.

The in vivo results with parent compounds (**III**) and (**IV**) were in agreement with their in vitro behaviors, poor capability to decrease parasitemia and to shift the peak of maximum parasitemia (for details see the corresponding section in Supporting Information Material, in vivo studies of parent compound (**III**) and (**IV**)). Additionally, some potential immune-suppressive properties in the treatment with the parent compounds were evidenced in the dose vs response studies (see Figure S5b in Supporting Information), as was

dx.doi.org/10.1021/jm500018m | J. Med. Chem. 2014, 57, 3984−3999

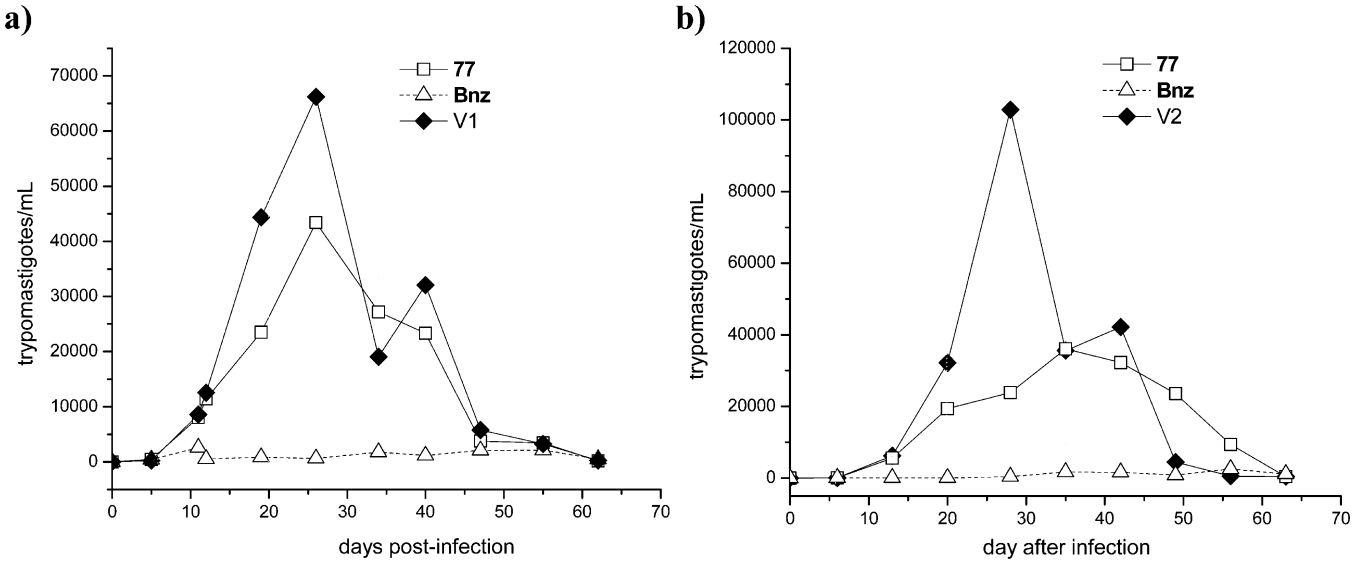

Figure 5. Parasitemia of mice treated with 107 μmol/kg b.w./day of **77** (□), group treated with 192 μmol/kg b.w./day of **Bnz** (△), and control group (♦). (a) **experiment 1**: compound **77** was suspended in V1 (n = 8/group). (b) **experiment 2**: compound **77** was suspended in V2 (n = 7/group). Highlighted regions (≡) correspond to the period of treatment (between days 6 and 20 postinfection).

Table 7. Summary of in Vivo Studies

experiment	treatment with	vehicle	doses (μmol/kg b.w./day)	peak of maximum parasitemia (day)	percentage of survival (%)[a]
1	V1			26	75
	Bnz	V1	192	55	100
	77	V1	107	26	75
2	V2			28	67
	Bnz	V1	192	56	100
	77	V2	107	35	100
3	V2			28	67
	Bnz	V1	192	56	100
	77	V2	214	35	100
4	V2			26	50
	Bnz	V1	192	42	100
	80	V2	107	42	100

[a]At the end of the studies (day 65).

previously observed, for nitrofuran analogues;[12a] this means significant parasitemia recrudescences were observed.

For the thiazoles, in the first approach (**experiment 1**) male BALB/c mice infected with CL Brener clone were treated orally, by intragastric gavage, during 14 days with derivative **77** (50 mg/kg b.w./day, 107 μmol/kg b.w./day) or **Bnz** (50 mg/kg b.w./day, 192 μmol/kg b.w./day), both in V1.[19b,25] The course of infection was monitored by counting blood parasites in a hemocytometer, and animal survival was followed for 65 days postinfection (Figure 5a and summary in Table 7). Because of the low stability in acid milieu, the very variable treatment vs response between mice (data not shown), and the low V1 suspension ability of compound **77**, we performed a second study (**experiment 2**) varying only the vehicle, using in this case the microemulsion V2. With this vehicle the intermouse results were more accurate and robust being the parasitemia and animal survival representative of the in vitro results (Figure 5b and summary in Table 7). In this condition, derivative **77** was able to delay the maximum of parasitemia shifting it 7 days relative to vehicle treated mice (Table 7). With this result, we selected V2 as formulation in the rest of the in vivo studies.

In a third experiment (**experiment 3**) the dose of derivative **77** was increased to 100 mg/kg b.w./day (214 μmol/kg b.w./day) closer to **Bnz** dose. In these conditions, derivative **77** was able to maintain the parasitemia of treated animals under the curve of untreated ones throughout the study period (Figure 6a). After day 35, the maximum of parasitemia for treated animals, the bloodstream form drops sharply. Additionally, in this case we determined the level of anti-*T. cruzi* antibodies at days 30 and 60 postinfection (Figure 6(b). Derivative **77** was able to significantly decrease, with respect to untreated animals, the antibodies at day 60. Furthermore, in this experiment the survival animals treated with **77** was 100% (summary in Table 7).

Lastly, derivative **80** was also in vivo evaluated (**experiment 4**) using similar conditions as those of **experiment 2**, i.e., vehicle V2 and orally administration of 50 mg/kg b.w./day (107 μmol/kg b.w./day). The modification involved a different treatment schedule, receiving the derivative **80** during 14 days, in a 19 day schedule with 4 days of resting and 5 days of administration followed by 2 days of rest, repeating this administration scheme two more times (Figure 7a). Even before the first peak of parasitemia derivative **80** appeared to

dx.doi.org/10.1021/jm500018m | J. Med. Chem. 2014, 57, 3984−3999

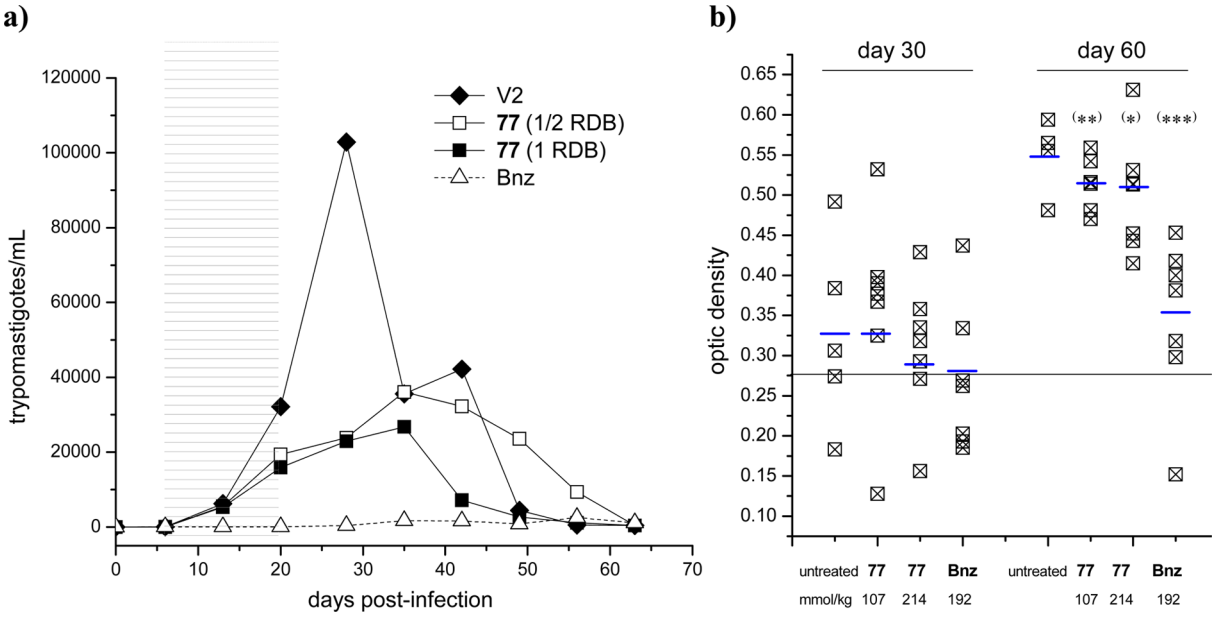

Figure 6. Results of in vivo **experiment 3**. (a) Parasitemia of mice (n = 7/group) treated with 107 (**experiment 2**, Figure 5a, and 214 μmol/kg b.w./day of 77, □ and ■, respectively), group treated with 192 μmol/kg b.w./day of **Bnz** (△), and control group (♦). (b) Anti-*T. cruzi* antibody levels at days 30 and 60. Lower line represents the cutoff (antibody levels for healthy animals). $^{(*)}$ $p < 0.10$, $^{(**)}$ $p < 0.05$, $^{(***)}$ $p < 0.01$, with respect to untreated animals (only V2). RDB: relative doses to **Bnz**.

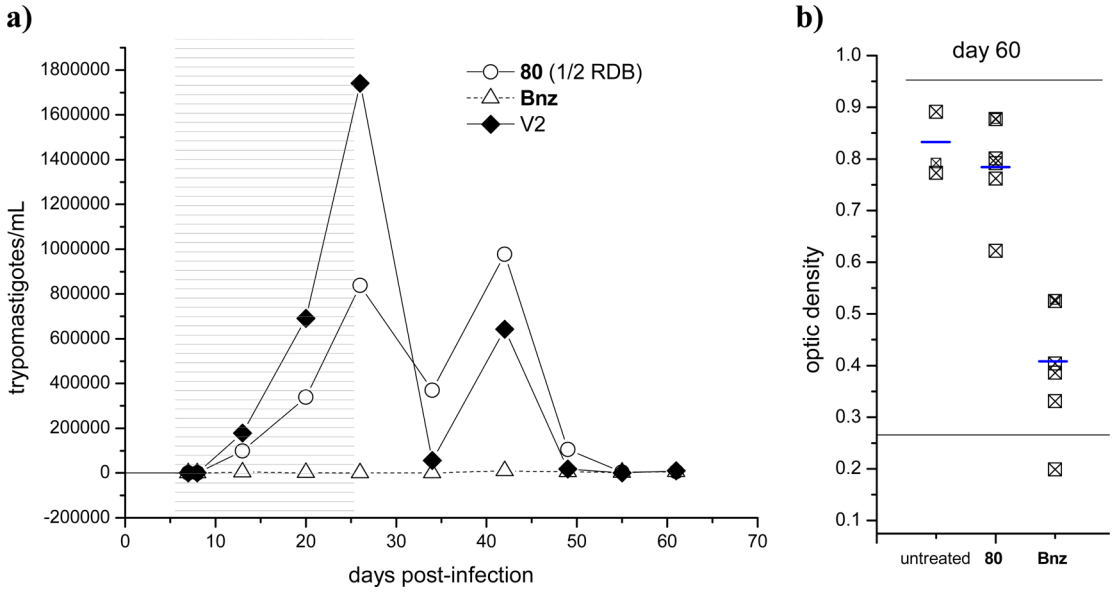

Figure 7. Results of in vivo **experiment 4**. (a) Parasitemia of mice (n = 6/group) treated with 107 μmol/kg b.w./day of **80** (○), group treated with 192 μmol/kg b.w./day of **Bnz** (△), and control group (♦). Highlighted regions (≡) correspond to the period of treatment schedule (between days 6 and 25 postinfection). (b) Anti-*T. cruzi* antibody levels at day 60. Lower line represents the cutoff (antibody levels for healthy animals).

work adequately, however, after passing the bloodstream valley (day 34) it was not able to keep the trypomastigotes below the corresponding levels for untreated animals. That may be the result of the administration schedule of derivative **80**, which could modify the amount of compound availability during the treatment in comparison with **Bnz** or derivative **77** administration schedules. Despite that the animal survival rate was 100% (Table 7), therefore, anti-*T. cruzi* antibodies were evaluated at day 60, which were not significantly different from the untreated control (Figure 7b).

■ DISCUSSION

We reported the in vitro biological activity against different forms of *T. cruzi* of 82 new compounds developed using compounds (**III**) and (**IV**) as partially- and nonmutagenic templates. Derivatives **3**, **6**, **7**, **11**, **40**, **77**, **78**, and **80** were the most active against epimastigotes Tulahuen 2 strain with **3**, **6**, **7**, **11**, and **77** at least 4 times more active than the template (**III**), **Nfx**, and **Bnz** (Tables 1−3).

Derivatives **3**, **11**, **62**, **77**, and **80** were also active against amastigotes Sylvio X-10 being **62**, **77**, and **80**, equipotent to **Nfx** (Table 4). Concommitantly, derivative **77** displayed activity against the circulating form of *T. cruzi*, trypomastigote

dx.doi.org/10.1021/jm500018m | *J. Med. Chem.* 2014, 57, 3984−3999

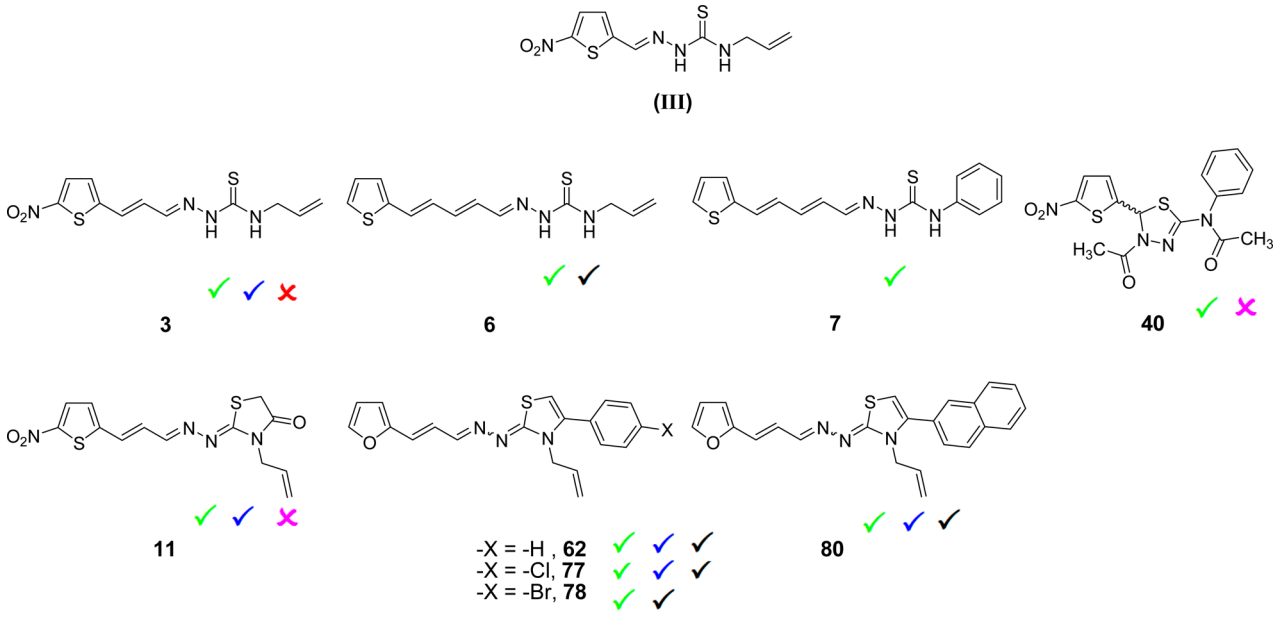

Figure 8. Summary of the tree-structural modifications performed and in vitro bioactivities obtained (green check, active against epimastigotes; blue check, active against amastigotes; red ×, mutagenic in both absence and presence of S9; pink ×, mutagenic in the absence or presence of S9; black check, nonmutagenic).

form. Along with these findings, derivatives **62**, **77**, and **80** also possess selectivity to *T. cruzi* (Table 4) being 5 times more selective than **Nfx** when Vero cell cytotoxicity was used as a comparison.

Among the compounds with the best antiparasitic activities (**3**, **6**, **7**, **11**, **40**, **62**, **77**, **78**, and **80**, Figure 8) the nitro derivatives **3**, **11**, and **40** displayed mutagenic effects in some of the experimental conditions, -S9 or +S9, while **62**, **77**, and **80** were not mutagenic in the Ames test against the five *S. typhimurium* strains recommended by OECD (Tables 6 and 7).

According to their biological behaviors, furan derivatives **77** and **80** were candidates (Figure 8) for pharmacological studies. Consequently, lead compounds were further evaluated for stability and solubility. Although, despite being salts, they displayed very poor solubility in aqueous milieu and they could be little stable in the gastrointestinal tract (Figure 4); therefore, it was decided to formulate them as microemulsions for in vivo studies. Microemulsioned systems could improve the solubility and stability of drugs,[23] in addition to becoming long-acting, increasing their bioavailability and decreasing its dose, and generating vectoring differential to certain tissues or organs in the body.

The pharmacological proofs of concept were done with parent compounds (**III**) and (**IV**) and derivatives **77** and **80**. The results of parent compounds were in agreement with the in vitro behavior. In the case of compound (**III**) the in vivo activity was adequate, in one of the conditions, but together with compound (**IV**) showed clear immune-suppressive behavior, evidenced by the exacerbation of the levels of the bloodstream forms, without modification in the anti-*T. cruzi* antibody levels. Moreover, the leads **77** and **80** displayed in vivo activity against the infected animals that probed the concept. In the in vivo **experiments 2**–**4**, the animals treated with them showed 100% survival rate at the end of the assays.

The blood study findings showed that derivative **77**, at a dose near to a half of the dose used for **Bnz** (**experiment 2**), exhibited a particular biological profile, shifting the parasitemia maximum to 7 days with respect to the control (Table 7) and abolishing the second maximum parasitemia peak that appeared in the untreated animals at day 42. These data clearly showed that thiazole **77** affected in vivo trypomastigotes, depleting the blood stream forms corroborated by the shifting of first parasitemia peak, and also the amastigote forms, corroborated by the absence of the second parasitemia peak. These results were in agreement with the values of anti-*T. cruzi* antibodies where derivative **77** showed significantly low levels at 60 days postinfection (Figure 6b).

However, derivative **80** was able to diminish the levels of bloodstream forms previous to the first parasitemia maximum peak, but after that levels were raised with respect to the untreated controls (Figure 7a). These data could indicate the lower in vivo effect of thiazole **80** on amastigotes that could be corroborated by the antibody level findings (Figure 7b); however, pharmacokinetic behavior of **80** different from **77** could not be ruled out.

From a chemical point of view, these compounds are synthesized by simple, scalable, and cost-effective procedures. In comparison to the reference drug or other compounds currently studied as anti-*T. cruzi* agents, our thiazoles have the following advantages (Table 8): (i) lower production cost and (ii) lower molecular complexities.

These good findings, i.e., absence of mutagenicity and in vivo activity, promote further thorough studies, modifying doses, administration routes, extending the in vivo treatment until after the maximum peak of parasitemia, and combinations with other drugs.

■ CONCLUSIONS

We have identified new thiazoles as excellent antitrypanosomatid agents. Observing the lack of mutagenic properties of them, the absence of toxicity, and the in vivo antitrypanosoma results, these compounds could be considered for further preclinical studies in order to generate new anti-Chagas drugs. Currently, we are performing studies related to identifying the mechanism of action (i.e., oxidative stress and squalene

dx.doi.org/10.1021/jm500018m | *J. Med. Chem.* 2014, 57, 3984−3999

Table 8. Summary of Production Characteristics of 77 Compared to Commercial Drugs

Cpd	price per g[a]	steps in the synthetic procedures	other observations
Bnz	104.0	3[b]	
ravuconazole[c]	350,000.0	more than 5	chiral centers
posaconazole[c]	300,000.0	more than 5	chiral centers
77	3.0[d,e]	2	geometric isomers
	2.6[e,f]	3	

[a]The price per gram of compounds were obtained from Sigma-Aldrich retail prices (http://www.sigmaaldrich.com/catalog) for **Bnz** or from http://www.scbt.com for **ravuconazole** and **posaconzale** and are expressed in $ (United States dollar). [b]From commercial 2-nitroimidazole. [c]Antifungal drugs recently used in clinical trials for the treatment of Chagas disease. [d]From furylacrolein. [e]Calculated only considering the reactants using retail prices of them (http://www.sigmaaldrich.com/catalog). [f]From furfural.

accumulation), pharmacokinetic studies, and new pharmacological schedules.

EXPERIMENTAL SECTION

Chemistry. All starting materials were purchased from Sigma-Aldrich Co. (USA) and Acros Organics (Janssen Pharmaceutical, Geel, Belgium). All solvents were dried and distilled prior to use. All the reactions were carried out in a nitrogen atmosphere. All of the synthesized compounds were chemically characterized by thin layer chromatography (TLC), nuclear magnetic resonance (^{1}H NMR, ^{13}C NMR), and elemental microanalyses (CHN). Alugram SIL G/UV254 (Layer: 0.2 mm) (Macherey-Nagel GmbH & Co. KG., Düren, Germany) was used for TLC, and silica gel 60 (0.040−0.063 mm, Merck) was used for flash column chromatography. The NMR spectra were recorded on a Bruker DPX 400 (400 MHz for ^{1}H and 100 MHz for ^{13}C), using TMS as the internal standard and with the indicated deuterated solvent; the chemical shifts are reported in ppm (δ) and coupling constants (J) values are given in Hertz (Hz). Signal multiplicities are represented by s (singlet), d (doublet), dd (double doblet), t (triplet), tt (triple triplet), and m (multiplet). Structural assignments were corroborated by HMBC and HSQC experiments. Mass spectrometry experiments were performed on a HEWLETT PACKARD MSD 5973 or a LC/MSD-Serie 100 using electronic impact (EI) or electrospray ionization (ESI), respectively. To determine the purity of the compounds, elemental microanalyses obtained on a Carlo Erba Model EA1108 elemental analyzer from vacuum-dried samples were used. The analytical results for C, H, and N were within ±0.4 of the theoretical values. Melting points were recorded on ELECTROTHERMAL IA-9100 equipment, and they were not corrected.

The measurements for single crystal derivative **77** were performed on an Oxford Xcalibur Gemini Eos CCD diffractometer with graphite-monochromated CuKα (λ = 1.54178 Å) radiation. X-ray diffraction intensities were collected (ω scans with ϑ and κ-offsets), integrated, and scaled with CrysAlisPro[26] suite of programs. Most of the diffraction pattern was interpreted in terms of two crystal domains (twins) related to each other through a rotation of 180° around the reciprocal b^* axis of the strongest diffracting crystal domain (hereafter, twin #1). The unit cell parameters for both twins were equal to within experimental accuracy. They were obtained by least-squares refinement based on the angular settings for all collected, nonoverlapping reflections with intensities larger than seven times the standard deviation of measurement errors using CrysAlisPro. The reflections were indexed in the reciprocal unit cell of the corresponding domain. Data were corrected empirically for absorption employing the multiscan method implemented in CrysAlisPro. The diffraction data indexed in the reciprocal unit cell of twin #1 (with about 62% of diffracting power) was employed to solve the structure by direct methods using SHELXS-97[27] and the corresponding molecular model developed by alternated cycles of Fourier methods and full-matrix least-squares refinement on F^2 with SHELXL-97.[28] Refinement showed evidence for the presence of strong overlap between reflections from both twins. Therefore, it was resorted to the data reduction of twin crystals facility implemented in CrysAlisPro to generate a data set including all the reflections from both domains with the overlapping ones flagged for further structure development (expansion) and refinement with SHELXL-97. With these data all hydrogen atoms were found in a difference Fourier map phased on the heavier atoms. However, the organic molecule H atoms were positioned stereochemically and refined with deriding model. The water H atoms were refined with isotropic displacement parameters at their found positions with Ow−H and H···H distances restrained to target values of 0.86(1) and 1.36(1) Å, respectively. The solid state molecular model of **77** was drawn with ORTEP.[29]

Appearances, yields, spectroscopic data, elemental microanalyses, and crystallographic data of the products are collected in the Supporting Information.

*General Procedure for the Preparation of Derivatives **1**−**7**, **46**, **49**−**51**, **54**, **55**, **63**, **67**, **69**, **70**, and **72**.* A mixture of the corresponding aldehyde (1.05 equiv), the corresponding thiosemicarbazide (1.00 equiv), catalytic amount of *p*-toluenesulfonic acid, and dry toluene (1 mL per 100 mg of aldehyde) was stirred at room temperature until disappearance of the aldehyde (12−24 h, checked by TLC, SiO_2, and petroleum ether/EtOAc 70:30). After that, the precipitate was filtered off and washed with petroleum ether. The solid was crystallized from ethanol.

*General Procedure for the Preparation of Derivatives **8**−**16**, **52**, **60**, **64**, and **73**.* A mixture of the corresponding thiosemicarbazide (1.0 equiv), ethyl bromoacetate (2.0 equiv), anhydrous sodium acetate (4.0 equiv), and dry ethanol (1 mL per 100 mg of thiosemicarbazide) was heated at reflux until disappearance of the thiosemicarbazide (4−10 h, checked by TLC, SiO_2, and petroleum ether/EtOAc 70:30). After that, the mixture was cooled at room temperature, and the precipitate was filtered off and washed with ethanol/water (80:20). The solid was crystallized from ethanol or ethanol/water.

*General Procedure for the Preparation of Derivatives **17**−**38**, **45**, **47**, **48**, **53**, **56**−**59**, **61**, **62**, **65**, **66**, **68**, **71**, **74**, and **76**−**80**.* A mixture of the corresponding thiosemicarbazide (1.0 equiv), the α-haloketone (2.0 equiv), and dry ethanol (1 mL per 100 mg of thiosemicarbazide) was heated at reflux until disappearance of the thiosemicarbazide (4−10 h, checked by TLC, SiO_2, and petroleum ether/EtOAc 70:30). After that, the mixture was cooled at room temperature, and the precipitate was filtered off and washed with ethanol/water (80:20). The solid was crystallized from ethanol or ethanol/water.

*Preparation of Derivative **75** Using Sodium Dithionite (via **1**).* A mixture of derivative **79** (0.1 g), sodium dithionite (0.7 g, added during 70 min in seven portions of 0.1 g), THF (10 mL), and water (10 mL) was stirred at reflux under nitrogen atmosphere for 8 h. After that, the solvent was evaporated in vacuo and the residue was partitioned between CH_2Cl_2 (30 mL) and aqueous sodium bicarbonate (5%, 2 × 15 mL). The organic layer was dried with anhydrous Na_2SO_4 and evaporated in vacuo. The desired product was purified by column chromatography (Al_2O_3 and petroleum ether/EtOAc 0 to 30%).

*Preparation of Derivative **75** Using Stannous Chloride (via **2**).* A mixture of derivative **79** (0.1 g), $SnCl_2$ (10 equiv), DMF (0.5 mL), catalytic amount of acetic acid, and dried toluene (10 mL) was stirred at 90 °C under nitrogen atmosphere for 2 h. After that, the solvent was evaporated in vacuo and the residue was partitioned between CH_2Cl_2 (30 mL) and aqueous sodium bicarbonate (5%, 4 × 15 mL). The organic layer was dried with anhydrous Na_2SO_4 and evaporated in vacuo. The desired product was purified by column chromatography (Al_2O_3 and petroleum ether/EtOAc 0 to 30%).

*General Procedure for the Preparation of Derivatives **39**−**42** and **81**.* A mixture of the corresponding thiosemicarbazide (1 equiv) and acetic anhydride (10 mL per mmol of thiosemicarbazide) was heated at reflux until disappearance of the thiosemicarbazide (2−4 h, checked by TLC, SiO_2, and petroleum ether/EtOAc 70:30). After that, the mixture was partitioned between EtOAc (30 mL) and aqueous sodium

dx.doi.org/10.1021/jm500018m | J. Med. Chem. 2014, 57, 3984−3999

bicarbonate (5%, 4 × 15 mL). The organic layer was dried with anhydrous Na_2SO_4 and evaporated in vacuo. The desired product was purified by column chromatography (SiO_2 and petroleum ether/EtOAc 0 to 40%).

*Preparation of Derivative **43***. A mixture of **3** (3 mmol) and ferric chloride (1.2 mmol) in anhydrous ethanol (3 mL) was heated at reflux for 8 h. After that, the mixture was partitioned between EtOAc (30 mL) and aqueous sodium bicarbonate (5%, 4 × 15 mL). The organic layer was dried with anhydrous Na_2SO_4 and evaporated in vacuo. The desired product was purified by column chromatography (SiO_2 and petroleum ether/EtOAc 0 to 40%).

Biology. *Antitrypanosomatid in Vitro Evaluation. Anti-T. cruzi in Vitro Test Using Epimastigotes of Tulahuen 2 Strain. Trypanosoma cruzi* epimastigotes (Tulahuen 2 strain) were grown at 28 °C in an axenic milieu (BHI-Tryptose) as previously described,[19] supplemented with 5% fetal bovine serum (FBS). Cells from a 5−7 day old culture (exponential phase) were inoculated into 50 mL of fresh culture milieu to give an initial concentration of 1×10^6 cells/mL. Cell growth was followed by measuring the absorbance of the culture at 600 nm every day. At day 5, the exponential phase of the growth, the parasites were inoculated with the indicated quantity of the drug from a stock solution in DMSO. The final concentration of DMSO in the culture milieu never exceeded 0.4%, and the control was run in the presence of 0.4% DMSO and in the absence of drugs. No effect on epimastigote growth was observed due to the presence of up to 1% DMSO in the culture milieu. Each compound concentration was evaluated in duplicate. The percentage of inhibition (PGI) was calculated as follows: PGI (%) = $\{1 - [(A_p - A_{0p})/(A_c - A_{0c})]\} \times 100$, where $A_p = A_{600}$ of the culture containing the drug at day 5; $A_{0p} = A_{600}$ of the culture containing the drug just after addition of the inocula (day 0); $A_c = A_{600}$ of the culture in the absence of drugs (control) at day 5; $A_{0c} = A_{600}$ in the absence of the drug at day 0. In order to determine IC_{50} values, 50% inhibitory concentrations, parasite growth was followed in the absence (control) and presence of increasing concentrations of the corresponding drug. At day 5, the absorbance of the culture was measured and related to the control. The IC_{50} value was taken as the concentration of drug needed to reduce the absorbance ratio to 50%.

Anti-T. cruzi in Vitro Test Using Amastigotes of Sylvio X-10 Strain.[30] VERO cells (ATCC), diluted to 3×10^5 cells/mL in RPMI 1640 milieu plus 10% hiFCS, were plated in 16-well Lab-tekTM tissue culture chamber slides (Life Technologies, Paisley, UK) and allowed to adhere for 24 h at 37 °C in a 5% CO_2/95% air mixture. Adherent cells were infected with tissue derived trypomastigotes (TDT) at a ratio of parasites to cells of 10:1. The cultures were maintained in a 5% CO_2/95% air mixture at 37 °C. TDT were obtained by successive serial infections in VERO cells with released parasites from culture supernatants. After 24 h, free parasites were removed by washing, and infected cultures were incubated for 72 h with 3-fold **Nfx** (0.3−87.0 μM) and **Bnz** (1.2−96.0 μM) and detest compounds (at five doses) for 5 days at 37 °C, in a 5% CO_2/95% air mixture. The cultures were then fixed with methanol and stained with Giemsa. Each compound concentration was evaluated in quadruplicate, and control cultures were maintained without drug. The results are the means of three independent experiments. Drug activity was determined by the percentage of infected cells in treated and untreated cultures by direct counting cells infected in a total of 300 cells using microscopy. Results were expressed as the biological activity concentrations 50 and 90 (IC_{50} and IC_{90}) by sigmoidal regression using XLfit4 software.

Anti-T. cruzi in Vitro Test Using Trypomastigotes of Y Strain.[19b,25] BALB/c mice infected with *T. cruzi* were used 7 days after infection. Blood was obtained by cardiac puncture using 3.8% sodium citrate as anticoagulant in a 7:3 blood/anticoagulant ratio. The parasitemia in infected mice ranged from 1×10^5 to 5×10^5 parasites/mL. The products, 77 and **Bnz**, were dissolved in minimal quantity of DMSO and added to PBS to give a final concentration of 25 μM. Aliquots (10 μL) of solution in triplicate were mixed in microtiter plates with 100 μL of infected blood containing parasites at a concentration near to 10^6 parasites/mL. Infected blood and infected blood containing gentian violet (GV) at 250 μg/mL concentration were used as control. The plates were shaken for 10 min at room temperature and kept at 4 °C for 48 h. Each solution was examined microscopically (OLYMPUS BH2) for parasite counting. The activity (% of parasite reduction) was compared with the untreated infected blood. Standard drug, GV, produced 100% reduction.

Nonspecific Mammalian in Vitro Cytotoxicity: VERO Cell Cytotoxicity Assay. The cytotoxicity against VERO cells (normal African green monkey kidney epithelial cells) at a maximum concentration of 2000 μM was determined for selected derivatives actives against the amastigote form of *T. cruzi*. The compounds dissolved in DMSO were evaluated at serial dilutions of the maximum concentration in fresh culture milieu. The culture was incubated at 37 °C, 5% CO_2 for 48 h. A negative control with DMSO (<0.1%) was included in each experiment. The percentage inhibition of cell growth was determined colorimetrically using Thiazole Blue (MTT; 3-[4,5-dimethylthiazol-2-y1]-2,5-diphenyltetrazolium bromide) (Aldrich, St. Louis MO) and reading of absorbance at 570 nm in a VersaMax Micro microplate reader. **Nfx** was used as positive control.

Red Blood Cell Lysis Assay.[31] Human blood collected in sodium citrate solution (3.8%) was centrifuged at 200*g* for 10 min at 4 °C. The plasma supernatant was removed and erythrocytes were suspended in ice cold PBS. The cells were again centrifuged at 200*g* for 10 min at 4 °C. This procedure was repeated two more times to ensure the removal of any released hemoglobin. Once the supernatant was removed after the last wash, the cells were suspended in PBS to 2% w/v red blood cell solution. A volume of 400 μL of compound to be analyzed, in PBS (final doses 50, 100, and 200 μM), negative control (solution of PBS), or AmpB (final dose 1.5 μM), was added to the 2% w/v red blood cell solution. Ten replicates for each concentration were done and incubated for 24 h at 37 °C prior to analysis. Complete hemolysis was attained using neat water yielding the 100% control value (positive control). After incubation, the tubes were centrifuged and the supernatants were transferred to new tubes. The release of hemoglobin into the supernatant was determined spectrophotometrically at 405 nm using an EL 301 MICROWELL STRIP READER. Results are expressed as percentage of total hemoglobin released in the presence of the compounds. This percentage was calculated using the equation percentage hemolysis (%) = $[(A_1 - A_0)/(A_{1water})] \times 100$, where A_1 is the absorbance at 405 nm of the test sample at $t = 24$ h, A_0 is the absorbance at 405 nm of the test sample at $t = 0$ h, and A_{1water} is the absorbance at 405 nm of the positive control (water) at $t = 24$ h. The experiments were done by quintuplicate. **AmpB** was used as positive control.

J774.1 Murine Macrophage Cell Cytotoxicity Assay. J774.1 murine macrophage cells (ATCC, USA) were grown in DMEM culture milieu containing 4 mM L-glutamine and supplemented with 10% heat-inactivated fetal calf serum. The cells were seeded in a 96 well plate (5×10^4 cells in 200 mL culture milieu) and allowed to attach for 48 h in a humidified 5% CO_2/95% air atmosphere at 37 °C. Afterward, cells were exposed for 48 h to the compounds (12.5−400.0 μM) or vehicle for control, and additional controls (cells in milieu) were used in each test. Three replicates for each concentration were done. Cell viability was then assessed by measuring the mitochondrial-dependent reduction of MTT to formazan. For this propose, MTT in sterile PBS (0.2% glucose) pH 7.4 was added to cells to a final concentration of 0.1 mg/mL and cells were incubated at 37 °C for 3 h. After removing the milieu, formazan crystals were dissolved in 180 mL of DMSO and 20 mL MTT buffer (0.1 M glycine, 0.1 M NaCl, 0.5 mM EDTA, 10.5 pH), and the absorbance at 560 nm was read using a microplate spectrophotometer. The IC_{50} is determined as the concentration that reduces absorbance by 50% compared to control treated with the solvent of the compounds and was determined by linear regression analysis.

"Hit-to-Lead" Phase Studies. Mutagenicity Assay. The method of direct incubation in plate was performed. Culture of *S. typhimurium* TA 98, TA 100, TA 102, TA 1535, and TA 1537 strains in the agar minimum glucose milieu-agar solution, Vogel Bonner E 50× and 40% glucose solution, was used. First, the direct toxicity of the compounds under study against the bacteria was assayed. DMSO solutions of studied compounds at five consecutive dilutions in third (starting at the highest doses without toxic effects) were assayed in triplicate.

dx.doi.org/10.1021/jm500018m | J. Med. Chem. 2014, 57, 3984−3999

Positive controls of 4-nitro-*o*-phenylendiamine (20.0 μg/plate, in the run without S9 activation) and 2-aminofluorene (10.0 μg/plate, in the cases of S9 activation) for TA98, 4-nitro-*o*-phenylendiamine (20 μg/plate, in the run without S9 activation) and 2-aminofluorene (10 μg/plate, in the run without S9 activation) for TA100, or sodium azide (2 μg/plate, in the run without S9 activation) and 2-aminoantracene (2 μg/plate, in the run without S9 activation) for TA102, TA1535, and TA1537 and negative control of DMSO were run in parallel. The influence of metabolic activation was tested by adding 500 μL of S9 fraction of mouse liver treated with Aroclor, obtained from Moltox, Inc. (Annapolis, MD, USA). The revertant number was counted manually. The sample was considered mutagenic when the number of revertant colonies was at least double that of the negative control for at least two consecutive dose levels.

Formulation Studies. Vehicle 1: composed of saline (80%) and Tween 80 (20%) (v/v). Formulation: compounds previously pulverized in a mortar were added to the V1, and the mixture was homogenized by a stirring system ultrasound chamber (ultasonic Cleaner, Hwashin instruments, sonic Power 405) for 10 min at maximum power; in some cases 10% DMSO was used. The resulting suspension was stirred gently for 24 h in a horizontal shaker.

Vehicle 2: composed of surfactant (10%), comprising Eumulgin HRE 40, sodium oleate, and soya phosphatidylcholine (8:6:3), oil phase (10%), comprising cholesterol, and phosphate buffer (pH = 7.4) (80%), according to Formariz et al.[23] with little changes. To prepare 10 mL of V2, 1.0 g of surfactant (460 mg polyoxyl-40 hydrogenated castor oil/Eumulgin HRE 40/360 mg of sodium oleate/180 mg of soya phosphatidylcholine), 1.0 g of cholesterol, and sufficient volume of phosphate buffer to 10 mL were used. Formulation: compounds, previously pulverized in a mortar, cholesterol, phosphatidylcholine, and polyoxyl-40 hydrogenated castor oil were dissolved in chloroform, and the solvent was evaporated under vacuum to dryness. To ensure complete removal of the chloroform, a stream of N_2 was passed for 5 min. In parallel, sodium oleate was dissolved in phosphate buffer and left for orbital shaking for 12 h at room temperature. This solution was then evaporated, and the mixture was homogenized and immersed in an ultrasonic bath at full power for 30 min; if it was not a homogeneous solution or did not have the desired consistency, it was reimmersed in an ultrasonic bath for another 30 min.

Stability Studies.[32] For pH stability study, we utilized the following aqueous solutions: (i) KCl·HCl buffer, pH 1.0; (ii) citrate buffer, pH 6.0; (iii) Tris·HCl buffer, pH 7.4, and (iv) borax·HCl buffer, pH 9.0. The stock solutions of compounds were prepared in DMSO, and the final concentration in the aqueous milieu was 1 mM. The solutions were further homogeneizated and incubated at 37 °C for 1 h. After that, thin layer chromatographies were done with the ethyl acetate extracts in order to confirm or discard the presence of decomposition products.

For the determination of liver fraction stability, we used rat liver microsomal and cytosolic proteins prepared following previously described methodology.[24] Briefly, homogenated livers were centrifuged for 30 min at 9000*g* at 4 °C; the pellet was discarded, and the supernatant was further centrifuged at 100 000*g* for 1 h at 4 °C. The pellet was discarded, and the supernatant fraction was further centrifuged at 100 000*g* for 1 h at 4 °C. The cytosolic and microsomal fractions, supernatant and pellet, respectively, were recovered. The pellet was washed twice by resuspension in the above Tris·HCl buffer solution, resedimented by centrifugation for 1 h at 100 000*g* at 4 °C, and finally resuspended in the Tris·HCl buffer solution. Metabolic assays were carried out with microsomes and cytosol either fresh or frozen in Tris·HCl buffer and stored at −80 °C. The protein content of the microsomal and cytosolic fractions was determined by the bicinchoninic acid assay from Sigma, as suggested by the manufacturer.

In Vivo Anti-T. cruzi Activity (Acute Model). BALB/c male mice (30 days old, 25−30 g) bred under specific pathogen-free conditions were infected by intraperitoneal injection of 10^3 blood trypomastigotes Y. One group of animals was used as control (inoculated orally with the vehicle V1 or V2), and two groups of animals were treated with each studied derivative and **Bnz**, respectively. First parasitemia was carried out 5 days postinfection (week 1), and the treatment began the following day (6th day). **Bnz** or derivative **77** was administered orally, using vehicle V1 or V2, at 50 or 100 mg/kg b.w./day, during 14 days. Derivative **80** was administered orally, using vehicle V2, at 50 mg/kg b.w./day according to the following administration-schedule: (i) 5 days of dosing; (ii) 2 days of resting; (iii) 5 days of dosing; (iv) 2 days of resting; (v) and finally 4 days of dosing. Parasitaemia in the control and treated mice was determined once a week after the first administration, for 60 days, in tail-vein blood; the mortality rate was recorded. All the sera obtained after centrifugation of the blood that was extracted from infected mice were tested twice by ELISA (enzyme linked immuno assay) at 30 and 60 days postinfection. A locally produced ELISA kit (Chagas test, IICS, Asunción, Paraguay) was used following the procedure recommended by the manufacturer (IICS Production Department, Asunción-Paraguay). The optical density values were obtained in an ELISA plate reader (Titerek Unistan I). Wilconxon test was used in order to compare the levels of anti-*T. cruzi* antibodies between experimental groups. The experimental protocols with animals were evaluated and supervised by the local Ethics Committee, and the research adhered to the Principles of Laboratory Animal Care.[33]

■ ASSOCIATED CONTENT

Supporting Information

Tree of decision in the design-process (Figure S1), NOE-diff experiments for both geometric isomers of derivative **22** (Figure S2), example of stability studies of acetyl-derivatives (Figure S3), relationship between activities against epimastigotes and amastigotes (Figure S4), cytotoxic behaviors against mammal cells (Table S1), in vivo biological results for **III** and **IV** derivatives (Figure S5, Table S2, and Figure S6), synthetic procedures and spectroscopic data for all developed compounds, crystal data, and structure refinement results for derivative **77** (Table S3), corresponding fractional coordinates and equivalent isotropic displacement parameters of the non-H atoms (Table S4), bond lengths and angles (Table S5), atomic anisotropic displacement parameters (Table S6), hydrogen atoms positions (Table S7), and hydrogen bond distances and angles (Table S8) This material is available free of charge via the Internet at http://pubs.acs.org.

Accession Codes

Crystallographic structural data for derivative **77** have been deposited at the Cambridge Crystallographic Data Centre (CCDC). Any request to the Cambridge Crystallographic Data Centre for this material should quote the full literature citation and the reference number CCDC 965369.

■ AUTHOR INFORMATION

Corresponding Authors

*(M.G.) Phone: 598 25258618 (ext. 216). Fax: 598 25250749. E-mail: megonzal@fq.edu.uy.
*(H.C.) Phone: 598 25250800. E-mail: hcerecetto@cin.edu.uy.

Notes

The authors declare no competing financial interest.

■ ACKNOWLEDGMENTS

The authors would like to thank the Comisión Sectorial de Investigación Científica (CSIC)-UdelaR (CSIC-*N*° 661) of Uruguay and the CONICET (PIP1529) and the ANPCyT (PME06 2804 and PICT06 2315) of Argentina. Collaborative work was performed under the auspices of the Iberoamerican Program for Science and Technology (CYTED), network RIDIMEDCHAG, Viceministerio de Ciencia y Tecnología (El Salvador), and Agencia Uruguaya de Cooperación Internacional (Uruguay). G.A., J.V., and Ma.Ga. thank ANII (Uruguay) for

their scholarships. G.A.E. and O.E.P. are Research Fellows of CONICET. M.C. thanks the Conselho Nacional de Desenvolvimento Científico e Tecnológico (CNPq, Brazil), Fundação de Amparo à Pesquisa do Estado de São Paulo (FAPESP), and Programa de Apoio ao Desenvolvimento Científico (PADC-FCF-UNESP) for a fellowship.

■ ABBREVIATIONS USED

Nfx, nifurtimox; Bnz, benznidazole; OECD, Organization for Economic Cooperation and Development; GV, gentian violet; V1, saline/Tween 80 (4:1, v:v); V2, microemulsion composed of cholesterol (10%) as oil phase, the surfactant (soya phosphatidylcholine/sodium oleate/polyoxyl-40 hydrogenated castor oil (3:6:8, 10%)), and phosphate buffer pH 7.4 (80%) as aqueous phase vehicle; RDB, relative doses to benznidazole; FBS, fetal bovine serum; BHI, brain and heart infusion; PGI, percentage of inhibition; TDT, tissue derived trypomastigotes; AmpB, amphotericin B

■ REFERENCES

(1) Dias, J. C.; Silveira, A. C.; Schofield, C. J. The Impact of Chagas Disease Control in Latin America: A Review. *Mem. Inst. Oswaldo Cruz* **2002**, *97*, 603−612.

(2) Schofield, C. J.; Jannin, J.; Salvatella, R. The Future of Chagas Disease Control. *Trends Parasitol.* **2006**, *22*, 583−588.

(3) World Health Organization/TDR. *Report of the Scientific Working Group on Chagas Disease, Buenos Aires 2005*; WHO: Geneva, Italy, 2006.

(4) (a) Magalhaes Moreira, D. R.; Manso Costa, S. P.; Zaldini Hernandes, M.; Montenegro Rabello, M.; Bezerra de Oliveira Filho, G.; Moutinho Lagos de Melo, C.; Ferreira da Rocha, L.; de Simone, C. A.; Salgado Ferreira, R.; Rodrigues Barbosa Fradico, J.; Santana Meira, C.; Teixeira Guimarães, E.; Mohan Srivastava, R.; Rêgo Alves Pereira, V.; Botelho Pereira Soares, M.; Lima Leite, A. C. Structural Investigation of Anti-*Trypanosoma cruzi* 2-Iminothiazolidin-4-ones Allows the Identification of Agents with Efficacy in Infected Mice. *J. Med. Chem.* **2012**, *55*, 10918−10936. (b) Gunatilleke, S. S.; Calvet, C. M.; Johnston, J. B.; Chen, C. K.; Erenburg, G.; Gut, J.; Engel, J. C.; Ang, K. K.; Mulvaney, J.; Chen, S.; Arkin, M. R.; McKerrow, J. H.; Podust, L. M. Diverse Inhibitor Chemotypes Targeting *Trypanosoma cruzi* CYP51. *PLoS Negl. Trop. Dis.* **2012**, *6*, e1736. (c) Recher, M.; Barboza, A. P.; Li, Z. H.; Galizzi, M.; Ferrer-Casal, M.; Szajnman, S. H.; Docampo, R.; Moreno, S. N.; Rodriguez, J. B. Design, Synthesis and Biological Evaluation of Sulfur-Containing 1,1-Bisphosphonic Acids as Antiparasitic Agents. *Eur. J. Med. Chem.* **2013**, *60*, 431−440. (d) Choi, J. Y.; Calvet, C. M.; Gunatilleke, S. S.; Ruiz, C.; Cameron, M. D.; McKerrow, J. H.; Podust, L. M.; Roush, W. R. Rational Development of 4-Aminopyridyl-Based Inhibitors Targeting *Trypanosoma cruzi* CYP51 as Anti-Chagas Agents. *J. Med. Chem.* **2013**, *56*, 7651−7668.

(5) (a) Cerecetto, H.; González, M. Synthetic Medicinal Chemistry in Chagas' Disease: Compounds at The Final Stage of "Hit-To-Lead" Phase. *Pharmaceuticals* **2010**, *3*, 810−838. (b) Guedes, P. M.; Silva, G. K.; Gutierrez, F. R.; Silva, J. S. Current Status of Chagas Disease Chemotherapy. *Expert Rev. Anti. Infect. Ther.* **2011**, *9*, 609−620. (c) González, M.; Cerecetto, H. Novel Compounds to Combat Trypanosomatid Infections: A Medicinal Chemical Perspective. *Expert Opin. Ther. Pat.* **2011**, *21*, 699−715.

(6) Cabrera, M.; Lavaggi, M. L.; Hernández, P.; Merlino, A.; Gerpe, A.; Porcal, W.; Boiani, M.; Ferreira, A.; Monge, A.; López de Cerain, A.; González, M.; Cerecetto, H. Cytotoxic, Mutagenic and Genotoxic Effects of New anti-*T. cruzi* 5-Phenylethenylbenzofuroxans. Contribution of Phase I Metabolites on the Mutagenicity Induction. *Toxicol. Lett.* **2009**, *190*, 140−149.

(7) (a) Hall, B. S.; Bot, C.; Wilkinson, S. R. Nifurtimox Activation by Trypanosomal Type I Nitroreductases Generates Cytotoxic Nitrile Metabolites. *J. Biol. Chem.* **2011**, *286*, 13088−13095. (b) Hall, B. S.; Wilkinson, S. R. Activation of Benznidazole by Trypanosomal Type I Nitroreductases Results in Glyoxal Formation. *Antimicrob. Agents Chemother.* **2012**, *56*, 115−123.

(8) (a) Gerpe, A.; Odreman-Nuñez, I.; Draper, P.; Boiani, L.; Urbina, J. A.; González, M.; Cerecetto, H. Heteroallyl-containing 5-Nitrofuranes as New Anti-*Trypanosoma cruzi* Agents with a Dual Mechanism of Action. *Bioorg. Med. Chem.* **2008**, *16*, 569−577. (b) Gerpe, A.; Álvarez, G.; Benítez, D.; Boiani, L.; Quiroga, M.; Hernández, P.; Sortino, M.; Zacchino, S.; González, M.; Cerecetto, H. 5-Nitrofuranes and 5-Nitrothiophenes with Anti-*Trypanosoma cruzi* Activity and Ability to Accumulate Squalene. *Bioorg. Med. Chem.* **2009**, *17*, 7500−7509.

(9) Aravena, M. A.; Olea, C.; Cerecetto, H.; González, H.; Maya, J. D.; Rodríguez-Becerra, J. Potent 5-Nitrofuran Derivatives Inhibitors of *Trypanosoma cruzi* Growth: Electrochemical, Spectroscopic and Biological Studies. *Spectrochim. Acta, Part A* **2011**, *79*, 312−319.

(10) Arbillaga, L.; San Miguel, L.; López, M.; Dávila, M. J.; Corcuera, L. A.; Gil, A. G.; Cerecetto, H.; González, M.; López de Cerain, A. Evaluation of the Genotoxicity of Nine Compounds with Significant in vitro Antichagasic Activity. *Toxicol. Lett.* **2010**, *196*, S169.

(11) *Test No. 471: Bacterial Reverse Mutation Test. OECD Guidelines for the Testing of Chemicals*. Section 4. The Organisation for Economic Co-operation and Development, 21-July 1997. http://www.oecd-ilibrary.org/environment/oecd-guidelines-for-the-testing-of-chemicals-section-4-health-effects_20745788 (accessed March 19, 2014).

(12) (a) Cerecetto, H.; Di Maio, R.; González, M.; Risso, M.; Sagrera, G.; Seoane, G.; Denicola, A.; Peluffo, G.; Quijano, C.; Stoppani, A. O. M.; Paulino, M.; Olea-Azar, C.; Basombrío, M. A. Synthesis and Antitrypanosomal Evaluation of *E*-Isomers of 5-Nitro-2-furaldehyde and 5-Nitrothiophene-2-carboxaldehyde Semicarbazone Derivatives. Structure-activity Relationships. *Eur. J. Med. Chem.* **2000**, *35*, 343−350. (b) Aguirre, G.; Cerecetto, H.; González, M.; Gambino, D.; Otero, L.; Olea-Azar, C.; Rigol, C.; Denicola, A. In vitro Activity and Mechanism of Action Against the Protozoan Parasite *Trypanosoma cruzi* of 5-Nitrofuryl Containing Thiosemicarbazones. *Bioorg. Med. Chem.* **2004**, *12*, 4885−4893. (c) Aguirre, G.; Cabrera, E.; Cerecetto, H.; Di Maio, R.; González, M.; Seoane, G.; Duffaut, A.; Denicola, A.; Gil, M. J.; Martínez-Merino, V. Design, Synthesis and Biological Evaluation of New Potent 5-Nitrofuryl Derivatives as Anti-*Trypanosoma cruzi* Agents. Studies of Trypanothione Binding Site of Trypanothione Reductase as Target for Rational Design. *Eur. J. Med. Chem.* **2004**, *39*, 421−431. (d) Aguirre, G.; Boiani, M.; Cabrera, E.; Cerecetto, H.; Di Maio, R.; González, M.; Denicola, A.; Sant'Anna, C. M. R.; Barreiro, E. J. New Potent 5-Nitrofuryl Derivatives as Inhibitors of *Trypanosoma cruzi* Growth. 3D-QSAR (CoMFA) Studies. *Eur. J. Med. Chem.* **2006**, *41*, 457−466.

(13) (a) Keskin, H.; Miller, R.; Nord, F. F. Studies of the Chemistry of Heterocyclics. XII.′ Preparation of Acetylenic Derivatives of Thiophene. *J. Org. Chem.* **1951**, *16*, 199−206. (b) Carrara, G.; Ettorre, R.; Fava, F.; Rolland, G.; Testa, E.; Vecchi, A. 4-Nitrocinnamic and *β*-(5-Nitro-2-thienyl)-acrylic Derivatives. *J. Am. Chem. Soc.* **1954**, *76*, 4391−4395.

(14) Omar, A.-M. M. E.; Chaaban, I.; AboulWafa, O. M.; Hassan, A. M.; Abou-Shleib, H.; Ismail, K. A. Novel Thiosemicarbazones, Thiazolines and Thiazolidines Derived from Chalcones: Synthesis, Antimicrobial and Anticancer Properties. *Alexandria J. Pharm. Sci.* **1989**, *3*, 211−216.

(15) (a) Medne, A. Y.; Saldabols, N. O. Synthesis and Transformations of Furan Derivatives. V. Synthesis of 4-Methylthiazolyl-(2)-hydrazones of Aldehydes and Ketones of the Furan Series. *Khim. Geterotsikl. Soedin.* **1965**, *1*, 629−631. (b) Bekhit, A. A.; Ashour, H. M.; Abdel Ghany, Y. S.; Bekhit, A.-D.; Baraka, A. Synthesis and Biological Evaluation of Some Thiazolyl and Thiadiazolyl Derivatives of 1*H*-Pyrazole as Anti-inflammatory Antimicrobial Agents. *Eur. J. Med. Chem.* **2008**, *43*, 456−463.

(16) Gerpe, A.; Boiani, L.; Hernández, P.; Sortino, M.; Zacchino, S.; González, M.; Cerecetto, H. Naftifine-analogues as Anti-*Trypanosoma cruzi* Agents. *Eur. J. Med. Chem.* **2010**, *45*, 2154−2164.

(17) (a) Faucher, J. F.; Baltz, T.; Petry, K. G. Detection of an "epimastigote-like" Intracellular Stage of *Trypanosoma cruzi*. *Parasitol. Res.* **1995**, *81*, 441−443. (b) Almeida-de-Faria, M.; Freymuller, E.; Colli, W.; Alves, M. J. *Trypanosoma cruzi*: Characterization of an Intracellular epimastigote-like Form. *Exp. Parasitol.* **1999**, *92*, 263−274.

(18) (a) Filardi, L. S.; Brener, Z. Susceptibility and Natural Resistance of *Trypanosoma cruzi* Strains to Drugs used Clinically in Chagas Disease. *Trans. R. Soc. Trop. Med. Hyg.* **1987**, *81*, 755−759. (b) Molina, J.; Brener, Z.; Romanha, A. J.; Urbina, J. A. In vivo Activity of the Bis-triazole D0870 Against Drug-susceptible and Drug-resistant Strains of the Protozoan Parasite *Trypanosoma cruzi*. *J. Antimicrob. Chem.* **2000**, *46*, 137−140.

(19) (a) Porcal, W.; Hernández, P.; Boiani, L.; Boiani, M.; Ferreira, A.; Chidichimo, A.; Cazzulo, J. J.; Olea-Azar, C.; González, M.; Cerecetto, H. New Trypanocidal Hybrid Compounds from the Association of Hydrazone Moieties and Benzofuroxan Heterocycle. *Bioorg. Med. Chem.* **2008**, *16*, 6995−7004. (b) Benitez, D.; Cabrera, M.; Hernández, P.; Boiani, L.; Lavaggi, M. L.; Di Maio, R.; Yaluff, G.; Serna, E.; Torres, S.; Ferreira, M. E.; Vera de Bilbao, N.; Torres, E.; Pérez-Silanes, S.; Solano, B.; Moreno, E.; Aldana, I.; López de Ceráin, A.; Cerecetto, H.; González, M.; Monge, A. 3-Trifluoromethylquinoxaline *N,N′*-Dioxides as Anti-trypanosomatid Agents. Identification of Optimal anti-*T. cruzi* Agents and Mechanism of Action Studies. *J. Med. Chem.* **2011**, *54*, 3624−3636. (c) Hernández, P.; Rojas, R.; Gilman, R. H.; Sauvain, M.; Lima, L. M.; Barreiro, E. J.; González, M.; Cerecetto, H. Hybrid Furoxanyl *N*-Acylhydrazone Derivatives as Hits for the Development of Neglected Diseases Drug Candidates. *Eur. J. Med. Chem.* **2013**, *59*, 64−74.

(20) Maron, D. M.; Ames, B. N. Revised Methods for the *Salmonella* Mutagenicity Test. *Mutat. Res.* **1983**, *113*, 173−215.

(21) (a) Chu, K. C.; Patel, K. M.; Lin, A. H.; Tarone, R. E.; Linhart, M. S.; Dunkel, V. C. Evaluating Statistical Analyses and Reproducibility of Microbial Mutagenicity Assays. *Mutat. Res.* **1981**, *85*, 119−132. (b) Claxton, L. D.; Allen, J.; Auletta, A.; Mortelmans, K.; Nestmann, E.; Zeiger, E. Guide for the *Salmonella typhimurium*/Mammalian Microsome Tests for Bacterial Mutagenicity. *Mutat. Res.* **1987**, *189*, 83−91.

(22) Sintov, A. C.; Shapiro, L. New Microemulsion Vehicle Facilitates Percutaneous Penetration in vitro and Cutaneous Drug Bioavailability in vivo. *J. Controlled Release* **2004**, *95*, 173−183.

(23) (a) Formariz, T. P.; Chiavacci, L. A.; Scarpa, M. V.; Silva-Júnior, A. A.; Egito, E. S.; Terrugi, C. H.; Franzini, C. M.; Sarmento, V. H.; Oliveira, A. G. Structure and Viscoelastic Behavior of Pharmaceutical Biocompatible Anionic Microemulsions Containing the Antitumoral Drug Compound Doxorubicin. *Colloids Surf., B* **2010**, *77*, 47−53. (b) Hu, L.; Yang, J.; Liu, W.; Li, L. Preparation and Evaluation of Ibuprofen-loaded Microemulsion for Improvement of Oral Bioavailability. *Drug Delivery* **2011**, *18*, 90−95. (c) Hu, L.; Jia, Y.; Niu, F.; Jia, Z.; Yang, X.; Jiao, K. Preparation and Enhancement of Oral Bioavailability of Curcumin using Microemulsions Vehicle. *J. Agric. Food Chem.* **2012**, *60*, 7137−7141. (d) Bshara, H.; Osman, R.; Mansour, S.; El-Shamy, A. H. Chitosan and Cyclodextrin in Intranasal Microemulsion for Improved Brain Buspirone Hydrochloride Pharmacokinetics in Rats. *Carbohydr. Polym.* **2014**, *99*, 297−305.

(24) Boiani, M.; Merlino, A.; Gerpe, A.; Porcal, W.; Croce, F.; Depaula, S.; Rodríguez, M. A.; Cerecetto, H.; González, M. *o*-Nitroanilines as Major Metabolic Products of anti-*Trypanosoma cruzi* 5-Phenylethenylbenzofuroxans in Microsomal and Cytosolic Fractions of Rat Hepatocytes and in Whole Parasitic Cells. *Xenobiotica* **2009**, *39*, 236−248.

(25) Boiani, M.; Boiani, L.; Denicola, A.; Torres de Ortiz, S.; Serna, E.; Vera de Bilbao, N.; Sanabria, L.; Yaluff, G.; Nakayama, H.; Rojas de Arias, A.; Vega, C.; Rolan, M.; Gómez-Barrio, A.; Cerecetto, H.; González, M. 2*H*-Benzimidazole 1,3-Dioxide Derivatives: A New Family of Water-Soluble Anti-Trypanosomatid Agents. *J. Med. Chem.* **2006**, *49*, 3215−3224.

(26) *CrysAlisPro*, version 1.171.36.20; Oxford Diffraction Ltd.: Abingdon, U.K., 2012.

(27) Sheldrick, G. M. *SHELXS-97*. Program for Crystal Structure Resolution; Univ. of Göttingen: Göttingen, Germany, 1997. See also: Sheldrick, G. M. *Acta Crystallogr.* **1990**, *A46*, 467−473.

(28) Sheldrick, G. M. *SHELXL-97*. Program for Crystal Structures Analysis; Univ. of Göttingen: Göttingen, Germany, 1997. See also: Sheldrick, G. M. *Acta Crystallogr.* **2008**, *A 64*, 112−122.

(29) Johnson, C. K. *ORTEP-II*. A Fortran Thermal-Ellipsoid Plot Program, Report ORNL-5318; Oak Ridge National Laboratory: Oak Ridge, TN, 1976.

(30) Luna, K. P.; Hernández, I. P.; Rueda, C. M.; Zorro, M. M.; Croft, S. L.; Escobar, P. In vitro Susceptibility of *Trypanosoma cruzi* Strains from Santander, Colombia, to Hexadecylphosphocholine (Miltefosine), Nifurtimox and Benznidazole. *Biomedica* **2009**, *29*, 448−455.

(31) (a) Fernandez, L.; Calderón, M.; Martinelli, M.; Strumia, M.; Cerecetto, H.; González, M.; Silber, J. J.; Santo, M. Evaluation of a New Dendrimeric Structure as Prospective Drugs Carrier for Intravenous Administration of Antichagasic Active Compounds. *J. Phys. Org. Chem.* **2008**, *21*, 1079−1085. (b) Merlino, A.; Benitez, D.; Chavez, S.; Da Cunha, J.; Hernández, P.; Tinoco, L. W.; Campillo, N. E.; Páez, J. A.; Cerecetto, H.; González, M. Development of Second Generation Amidino-hydrazones, Thio- and Semicarbazones as *Trypanosoma cruzi*-inhibitors Bearing Benzofuroxan and Benzimidazole 1,3-Dioxide Core Scaffolds. *Med. Chem. Commun.* **2010**, *1*, 216−228. (c) Merlino, A.; Benitez, D.; Campillo, N. E.; Páez, J. A.; Tinoco, L. W.; González, M.; Cerecetto, H. Amidines Bearing Benzofuroxan or Benzimidazole 1,3-Dioxide Core Scaffolds as *Trypanosoma cruzi*-Inhibitors: Structural Basis for their Interactions with Cruzipain. *Med. Chem. Commun.* **2012**, *3*, 90−101.

(32) Kerns, H. E.; Li, D. *Drug Like Properties: Concepts, Structure, Design and Methods. From ADME to Toxicity Optimization*; Academic Press: Oxford, U.K., 2008; pp 353 − 358.

(33) Morton, D. B.; Griffiths, P. H. M. Guidelines on the Recognition of Pain, Distress and Discomfort in Experimental Animal and a Hypothesis for Assessment. *Vet. Rec.* **1985**, *116*, 431−436.